COE-C3010 Computational Engineering Project

Project Report

In-situ experiments and mechanism-based modeling of the hydrogen-induced damage for steels

Group members: Hyeju Lee (781895), Laura Ikonen (785707), Sayoojya Prasad (791364)

School of Engineering, Aalto University

Advisor: Ms. Jiaojiao Wu

Supervisor: prof. Junhe Lian

Table of Contents

1. Abstract

It is well known that hydrogen can have a huge deteriorating effect on the mechanical properties of materials, especially high strength steels. Through this project, we wish to better understand the hydrogen embrittlement process. The aim of this project is to model a coupled hydrogen diffusion and stress modeling using the finite element method approach in Abaqus. But before this, we need to understand how hydrogen can diffuse through the material, which is the prime focus in the results of this project report. The project follows a hybrid methodology, containing both experimental and numerical parts. The aim of experimental study is to introduce hydrogen in the material through the hydrogen pre-charging tests, and measure the hydrogen concentration through the thermal desorption spectroscopy method. Finally, we conduct the in-situ hydrogen charging tensile tests to further understand how hydrogen influences the mechanical properties of the material. The simulation strategy aims to understand the underlying process of how hydrogen diffuses through the material by analyzing the diffusion equation. Firstly, three simulation strategies for simple diffusivity in one dimensional case are presented. We implemented an analytical approach solving the diffusion partial differential equation using the Crank-Nicholson method. Afterword, by making use of the analogy between the diffusion and heat transfer equations, we achieved the same results in Abaqus, confirming that our assumptions and approach in both cases were correct. Furthermore, we developed another simulation strategy in Abaqus with the mass flux concept, in order to get results that resembled the real-life experimental scenario. Then, we applied the two Abaqus simulation strategies also to three-dimensional complex geometries, proving that our simulation workflows can be applied to all cases.

2. Introduction

Hydrogen is known to have a deteriorating impact on the mechanical properties of certain materials. There is plenty of evidence provided in literature that supports this claim, further adding that hydrogen leads to degradation of ductility and brittle fracture, especially in high strength steels [1-4]. This poses a challenge for structures that are exposed to hydrogen like oil and gas structures, gearboxes, anchors of offshore wind turbines or even architectural constructions made of steel [5]. There have been incidents in the past, where hydrogen embrittlement has caused great structural damage. For example, 6 months prior to the opening of Oakland Bay Bridge, the east span of the bridge failed during testing, and a large number of shear bolts failed after only two weeks of service. This damage is likely caused by hydrogen embrittlement owing to the harsh environments the bridge is exposed to [5].

Therefore, while it is proven that hydrogen embrittlement indeed poses a threat, research is ongoing to understand the mechanism of how it happens. The two most investigated mechanisms include hydrogen induced decohesion (HID) and hydrogen enhanced local plasticity (HELP) [6]. One of the main issues is that owing to the small size of hydrogen, it can easily diffuse through the material and be found at several locations like voids, dislocations, vacancies, grain boundaries and so on. Hydrogen contributes to the build-up of enormous pressure at these locations, which causes the loss in ductility and finally leads to brittle failure.

This project follows a hybrid methodological approach, with both experimental and numerical tasks to understand this phenomenon better. Experimental tasks include hydrogen pre-charging of the specimen followed by thermal desorption spectroscopy test to measure the total hydrogen concentration. Furthermore, there is the in-situ hydrogen charging and tensile testing, where the specimen is exposed to hydrogen environment while it undergoes tensile testing. Experimental studies show us what happens in real life and provides us with valuable results. However, in order to understand the underlying mechanism and the process by which hydrogen embrittlement takes place, we need a computational approach to simulate various models. Numerical methodologies aiming to investigate the proposed mechanisms can

provide results that can be compared with experimental data. This combined approach will give a better overall picture to characterize the behaviour of various materials.

The big picture aim of the simulation method is to trace the local hydrogen concentration within the material for in-situ hydrogen charging tensile tests. This purpose calls for a coupled hydrogen diffusion and stress modelling using the Finite Element Method approach in Abaqus software along with the user subroutine.

However, before implementing the couple simulation strategy, it is important to understand how hydrogen diffuses through the material by investigating the diffusion equations in detail. This marks the scope of this project. Various specimen geometries were considered, and the diffusion of hydrogen through these specimens was studied using MATLAB as well as Abaqus. The similarity between the diffusion equation and heat transfer equation was made use of to conduct the simulations. The content of this paper is as follows. First, we give an extensive report on the theoretical background and literature review followed by a detailed explanation of the methodology. The paper presents the results and discussion of the simple diffusivity case for simple geometry, using three different numerical approaches. We further present cases of complex geometries as well. The results achieved from this study are promising and serves as a foundation for further studies and investigations in this field.

3. Literature Review / Theoretical Background

3.1 Hydrogen Embrittlement Understood

3.1.1 Overview

In today's world, hydrogen embrittlement is an important challenge to overcome. This phenomenon affects almost all high strength materials, most commonly steel and its alloys. Research is ongoing to learn more about the mechanisms of hydrogen embrittlement, but currently there is no method to completely prevent it from happening, or to manufacture materials that is insusceptible to this phenomenon. [7]

In simple words, hydrogen embrittlement can be defined as the embrittlement of a material by atomic hydrogen, due to the ingress of hydrogen into the material [8] – [10]. The material, once hydrogen ingresses into it, fails at a level much lower than when it is free of hydrogen. Hydrogen embrittlement can heavily reduce the ductility and load bearing capacity of the material eventually leading to cracking and brittle failure at stresses below the yield stress. Some examples of hydrogen embrittlement include cracking of weldments or hardened steels when they are exposed to conditions that lead to the introduction of hydrogen into the material. The materials most vulnerable to hydrogen embrittlement are high strength steels, and alloys of titanium and aluminum [11] [12].

3.1.2 Process of Hydrogen Embrittlement

Consider the situation where the hydrogen reduction, which is a cathodic reaction, occurs on the surface of a corroding metal, which is an anodic reaction. [7]

We have,

$$H^+ + e^- \rightarrow H_{(ads)} \qquad (1)$$

The hydrogen atoms are created and then adsorbed on the surface of the metal. Then, there are two possibilities. The hydrogen atoms can either combine to form hydrogen molecules and can then diffuse away from the surface. Or, they can dissolve into the metal to form adsorbed hydrogen in the interior of the metal. In the second case, the

hydrogen atoms once dissolved inside the metal, they accumulate at the internal imperfections like voids, where they combine to form hydrogen molecules: [13] - [15]

$$2\ H_{(ads)} \rightarrow H_2 \qquad (2)$$

In this way, all the hydrogen formed leads to the buildup of enormous pressure in the voids (almost thousands of atmospheres), causing the void to become a cavity and finally a blister forms near the metal surface. This enormous pressure can initiate large cracks. Thus, when some stress is applied on this metal, it does not bend as a ductile metal would, but rather it fractures along the ends. This means that the hydrogen has embrittled the metal [10]. Figure 1 illustrates the process of hydrogen blistering and embrittlement.

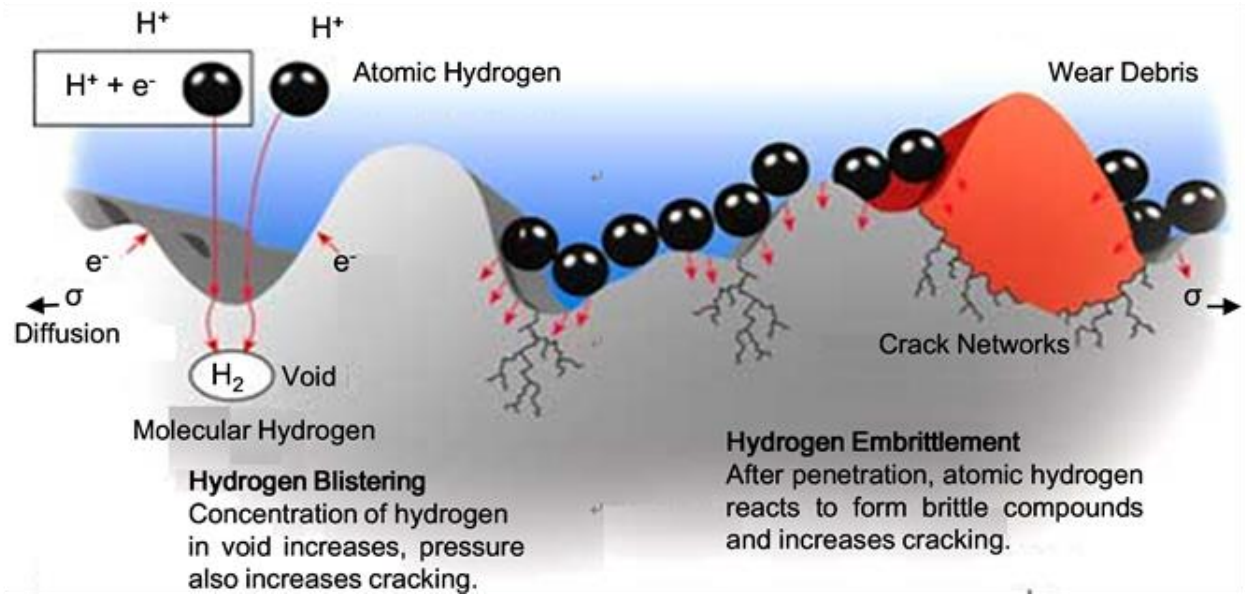

Figure 1: Schematic diagram of the process of hydrogen embrittlement [8]

One thing to note is that hydrogen embrittlement is not necessarily a permanent of process. Ductility can be restored in the material if the surrounding conditions are changed in a way that no more produces hydrogen on the surface, and all the hydrogen rediffuses from the metal [7].

3.2 Literature Review on Hydrogen Embrittlement

3.2.1 Overview

The first paper on hydrogen embrittlement of metals was published by Johnson [16] in 1875 as he observed the mechanical properties of iron that had been immersed in various acids. After a short time in the acids, the iron piece, that was able to bend many times, was bent once and then broke. He noted that this phenomenon is caused by hydrogen instead of acid. This was shown to be only a temporary effect since the metal regained its original properties over time [16].

Recent studies are revealing more and more information about the topic, for example, Wang's study [17] in 2012 proved the direct relationship between the diffusion coefficient of grades and fracture time [17]. However, even with potential harmful effects that can be caused by hydrogen embrittlement, the precise reasons and process remain not completely clear.

3.2.2 Proposed Mechanisms

Various studies have indicated that hydrogen has a huge effect on the mechanical properties of a metal. Hydrogen can degrade several properties of high strength steels like ductility, strength, and toughness, which leads to intergranular brittle fracture. However, the mechanism that is responsible for this embrittlement is not yet confirmed. There is a growing realization that hydrogen embrittlement is a complex, material, and environmental phenomenon, and that no one mechanism works for all. Out of proposed mechanisms, hydrogen-enhanced decohesion and localized plasticity mechanisms can be introduced here as they are frequently invoked [6].

Hydrogen-enhanced decohesion relies on the fact that hydrogen in the lattice reduces the bond strength, which leads to rupture at lower stress levels. In an attempt to understand how hydrogen changes the bond strength, computational simulation was utilized. Wang *et al.* [18] showed how hydrogen reduced cohesion of grain boundaries in Fe.

The hydrogen enhanced local plasticity (HELP) mechanism suggests that hydrogen improves the dislocation mobility. Thus, hydrogen reduces the stress needed to move a dislocation through various obstacles. Experimental studies of Robertson have helped support this mechanism [19].

Birnbaum and Sofronis [20] developed a hydrogen shielding concept to explain hydrogen's increase in mobility of dislocations. This became the basis for the hydrogen-enhanced localized plasticity mechanism of hydrogen embrittlement. The effect of hydrogen being segregated to elastic obstacles, and to the dislocation fields is studied in the shielding concept. The hydrogen alters the stress field where it is attached to. If in dislocation, the stress field will be increased in certain directions, and decreased in others, resulting in the hydrogen to move with less stress under some conditions.

3.2.3 Beachem’s discovery

In 1972, Beachem [21] recognized that the ductile features evident on hydrogen-induced failure surfaces reflected hydrogen enhancing plasticity processes. Only established on a posteriori interpretation of ductile features on failed surfaces in terms of plasticity, this interpretation was based neither on direct understanding of surface microstructure nor on evidence of hydrogen effect on the plasticity. A major turning point in the field of understanding hydrogen embrittlement mechanisms was reached with these assertions. Prior explanations assumed that ductile features visible on fracture surfaces were simply a byproduct of embrittlement, therefore irrelevant with respect to the mechanism [22–24]. Beachem's interpretations are significant because it has now been shown that the features on fracture surfaces cannot be used to determine the exact failure mode or path of failure.

3.3 Diffusion Equation

In order to study the mechanisms explained in 3.1.2 more clearly, it is important to understand how hydrogen diffuses inside a material by analyzing the diffusion equation. This understanding must then be coupled with the mechanical constitutive response of the material. [6]O. Barrera et al. have used the Abaqus software to try and solve the

coupled hydrogen diffusion-mechanics problem. Their aim is to better understand the HELP mechanism.

3.3.1 Fick's Laws of Diffusion

Hydrogen diffuses through the material obeying the Fick's laws of diffusion. There are two main types of diffusion- steady state diffusion and non-steady state diffusion. In steady state diffusion, the concentration gradient remains constant with time, and this process is explained by Fick's first law [25]:

$$J = -D \frac{d\varphi}{dx} \qquad (3)$$

Where,

$J = diffusion\ flux$

$D = diffusion\ coefficient$

$\varphi = concentration$

$x = position$

Secondly, there is the non-steady state of diffusion in which there is a temporal dependence, i.e., the concentration gradient varies with time. This phenomenon is governed by Fick's second law of diffusion [25]:

$$\frac{\partial \varphi}{\partial t} = D \frac{\partial^2 \varphi}{\partial x^2} \qquad (4)$$

Where,

$\varphi = concentration$

$t = time$

$D = diffusion\ coefficient$

$x = position$

The Fick's second law is derived from the Fick's first law. This is a partial differential equation that can be solved by using the appropriate boundary conditions.

3.3.2 Analogy with Heat Transfer Equation

The hydrogen diffusion equation is analogous to the heat equation, the latter can be easily implemented on Abaqus using the UMATHT subroutine. Owing to their size,

hydrogen atoms can diffuse through a metal very easily, by normal interstitial site (NILS) diffusion or dislocation transport. Trapped hydrogen at defects, even shallow defects can have a significant impact on the diffusion process. It is also assumed that a local equilibrium state between the mobile and trapped hydrogen populations is achieved. Hence, the hydrogen diffusion model is modified to include a factor depending on the strain rate. This ensures that the hydrogen concentration at lattice sites reduces as the trap sites are filled up [6].

Since the hydrogen diffusion equation is analogous to the heat transfer equation, we can use this fact to run the coupled hydrogen diffusion-mechanics simulations. The summary of this analogy is presented in Table 1 [6]. The degree of freedom in the heat transfer equation is temperature, whereas in the hydrogen diffusion equation it is C_L, or the hydrogen concentration in the lattice.

Heat equation	Mass diffusion equation
$\rho c_P \frac{\partial T}{\partial t} + \nabla \cdot \mathbf{J}_q + r_q = 0$	$\frac{C_T}{\partial t} + \nabla \cdot \mathbf{J}_m + r_m = 0$
Derivative of thermal energy per unit mass $\dot{U}_q = c_P \frac{\partial T}{\partial t}$	Derivative of total H concentration $\frac{\partial \bar{C}_T}{\partial t} = \frac{\partial (\bar{C}_L + \bar{C}_X)}{\partial t}$
Degree of freedom: temperature T	Degree of freedom: lattice H concentration $\bar{C}_L$
Heat flux: $\bar{\mathbf{J}}_q$	Hydrogen flux: $\mathbf{J}_m = \frac{D_L \bar{C}_L V_H}{RT} \nabla \sigma_H - D_L \vec{\nabla} \bar{C}_L$
Heat source: r_q (assume $r_q = 0$)	Hydrogen source: r_m (assume $r_m = 0$)
density: ρ	1 Unity

Table 1: Analogy of variables in heat transfer and diffusion equations [6]

There are three numerical solutions analyzed in [6]. The first is the pure diffusion case where the solution to a simple 1D diffusion problem is given, which can also be compared with the analytical solution. The second is an elastic diffusion 2D problem where complex geometries are used and finally, the third solution is the coupled elasto-plastic diffusion problem, which is done to analyze and understand the HELP mechanism as described earlier.

From the results, it was analyzed that hydrogen has a tendency to accumulate in areas with high local hydrostatic stress. Although, a high concentration of hydrogen leads to softening of the material, which implies a lower yield strength and hence a low hydrostatic stress. Thus, the process is self-regulating leading to an equilibrium between hydrostatic stress, hydrogen concentration and yield strength [6].

4 Experiments/Numerical methods

4.1 Material

In the project, the focus is on bainitic steels with superior strength, for example, CP1000. This material belongs to the advanced high strength steels (AHSS) with complex phase constituents. Because of their high strength and good ductility, they are commonly used in industries in order to achieve weight reduction. They normally consist of different phases like bainite, austenite, martensite, and so on. Figure 2 shows the microstructure of CP1000 steel which is obtained by scanning electron microscopy (SEM) technique of IEHK institute in RWTH Aachen University.

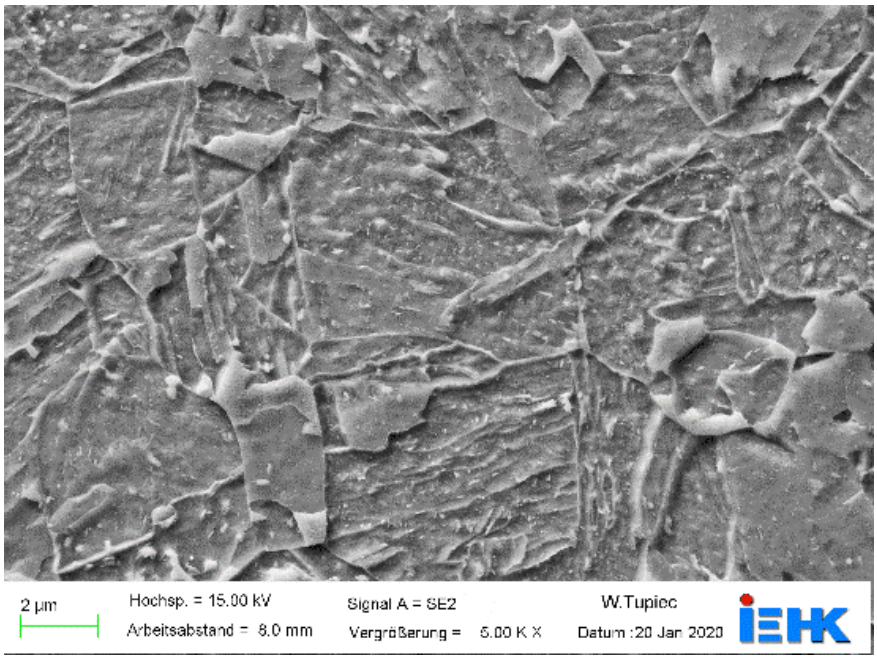

Figure 2: microstructure of CP1000 steel

Table 2 presents the chemical composition of CP1000 steel.

	C	Si	Mn	Cr	Ni	Mo	Cu	Al	Ti	V	Nb
wt%	0.119	0.261667	2.1773	0.234	0.023	0.013	0.02	0.047	0.029	0.0055	0.006

Table 2: Chemical composition of CP1000 steel

4.2 Experiments

4.2.1 Hydrogen Pre-charging

Hydrogen pre-charging is the process used to introduce hydrogen into the specimen through an electrochemical process. The electrolytic process, where low voltages are used to create reactions in solution, can be used to split water into hydrogen and oxygen. For the hydrogen pre-charging in our project, the solution environment 3% NaCl + 0.1% NH_4SCN was used. This chemical solution provides a weak acidic environment that lets the H^+ ions be diffused into the cathode, which in this case is the specimen surface. The chemical solution is prepared by 2 L deionized water + 60 g NaCl + 2 g NH_4SCN. NaCl is the electrolyte, and NH_4SCN or ammonium thiocyanate is a well-known catalyst in the electrical hydrogen charging methods [26]. Figure 3 shows the different steps and the specimen used in the hydrogen pre-charging step.

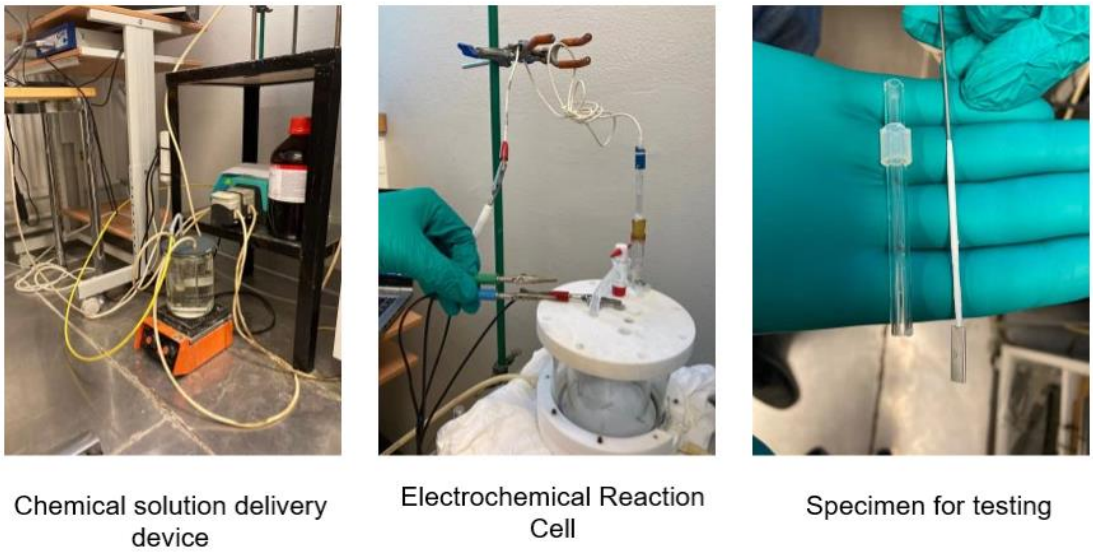

Figure 3: Hydrogen pre-charging set-up

4.2.2 Thermal Desorption Spectroscopy

Thermal desorption spectroscopy (TDS) is the method of measuring the hydrogen concentration in metallic materials.

The material used is CP1000 as described in 4.1. The specimen was cut using a sample cutting machine with a feed speed of 0.015 mm/s. Then, the specimen surface

was ground using sandpaper of brand number P1200, followed by cornering the specimen sides using sandpaper of brand number P800 to avoid any delivering problems in TDS measurement. Finally, the sample was weighed to record the mass which should be input into the program before the TDS measurement begins. The size of the TDS specimens was 15mm x 4mm x 1mm. Then, after the hydrogen pre-charging as explained in 4.2.1, the hydrogen content is measured using the TDS technique. [27]

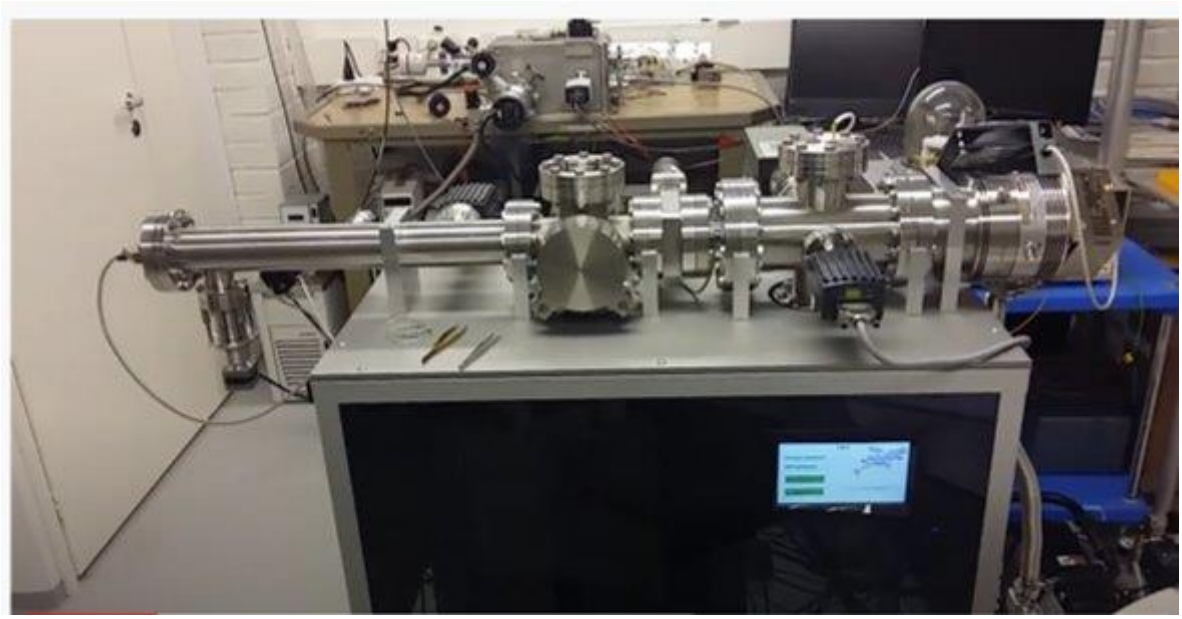

Figure 4: Experimental set-up of the TDS experiment

A schematic diagram of the TDS setup is shown in Figure 5 [27]. The concept, design, and construction of the apparatus were done at Aalto University in Espoo, Finland. The mass spectrometer and vacuum pumps were bought from Agilent Technologies, California, United States. The UHV measurement chamber is constantly held under a continuous vacuum pumping at 5 x 10^{-7} Pa. Before the transfer of the specimen to the measurement chamber, the specimen exchange and preliminary vacuum pumping are done using the AVC. An intermediate pressure of 10^{-4} Pa is required for the transportation of the specimen to the UHV measurement chamber in a safe and contamination-free manner. The preliminary pumping takes around 15 minutes in order to reach this intermediate pressure. This time is called ‘AVC dwell time’. The AVC is fitted with a specimen’s cooling system in order to reduce the hydrogen loss during the AVC dwelling time. A heatsink was attached to the specimen holder to provide heat transfer from the specimen. Figure 6 shows the schematic diagram of the cooling

system coupled to the AVC. The cooling agent used is liquid nitrogen. An automatic electronic unit controls the heatsink temperature. This gives a specimen cooling rate of 10 K / min with an accuracy of ±2 K [27]

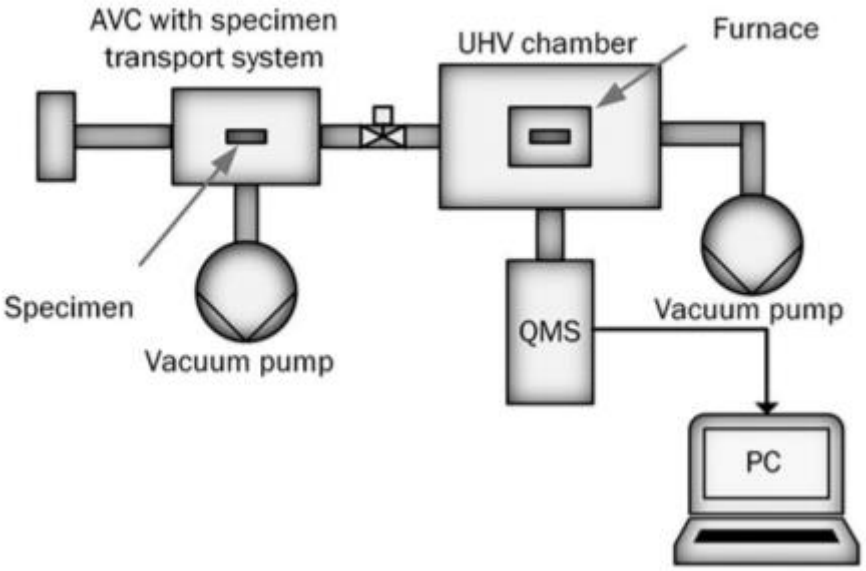

Figure 5: Schematic view of the TDS apparatus [27].

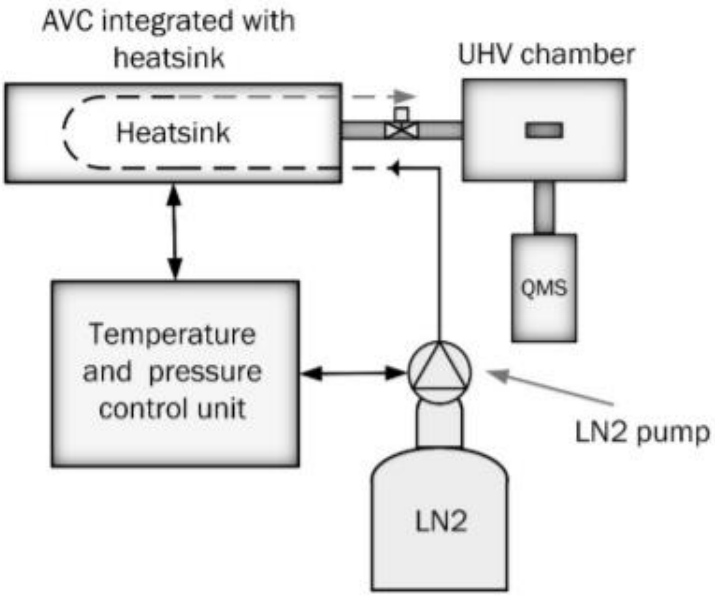

Figure 6: Schematic view of the AVC-coupled cooling system [27]

The AVC-coupled cooling system cooled down the specimens to 213 K and this cooling continued throughout the AVC dwelling time until the specimen was transferred to the UHV chamber for measurement. The TDS measurement was done at a heating rate of 10 K / min from room temperature to 1070 K. Finally, after

measurement, the hydrogen concentration in the specimen can be calculated by integrating the area under the TDS curve [27].

4.2.3 In-situ Hydrogen Charging Tensile Tests

In the in-situ hydrogen charging tensile tests, we use the tensile test machines to apply uniaxial loading on the specimen, while immersing the specimen in the hydrogen charging cell. So, the hydrogen charging and the tensile tests occur at the same time.

The purpose of doing this test is to understand how hydrogen influences the mechanical properties of the specimen. While the specimen is under the tensile testing, the dislocation density increases with increasing strain. The specimen will initially be in the elastic range, followed by the plastic range until crack initiation, which is preferred to happen at an area of high strain concentration. Further, the process continues with crack propagation until the specimen finally fractures. We expect that hydrogen accumulates in areas of high strain concentration, so hydrogen concentration is high at the crack initiation site. Conducting the in-situ hydrogen charging tensile tests will distinctly show us how hydrogen affects the crack propagation since hydrogen would increase the pressure at the internal voids, increasing the risk of crack-tip opening.

In this project, we start with hydrogen pre-charging for about 30 minutes, which will help reach the saturated state in the specimen, leading to a uniform concentration of hydrogen throughout the sample. This will be followed by the in-situ hydrogen charging tensile tests, and expect a non-uniform hydrogen concentration in the sample. This experimental strategy can give us valuable results for comparison with numerical simulations.

4.3 Calculation of Total Hydrogen Concentration from TDS Experiments Using MATLAB

4.3.1 Aim

The goal is to calculate the total hydrogen concentration inside the sample, which can be obtained from how much hydrogen was desorbed during the TDS test. The original data from the TDS experiment can be shown in a hydrogen pressure vs. temperature curve. As the temperature increases and hydrogen diffuses out of the sample, it affects

the pressure. This curve can then be recalculated and transformed to form hydrogen desorption rate vs. temperature curve.

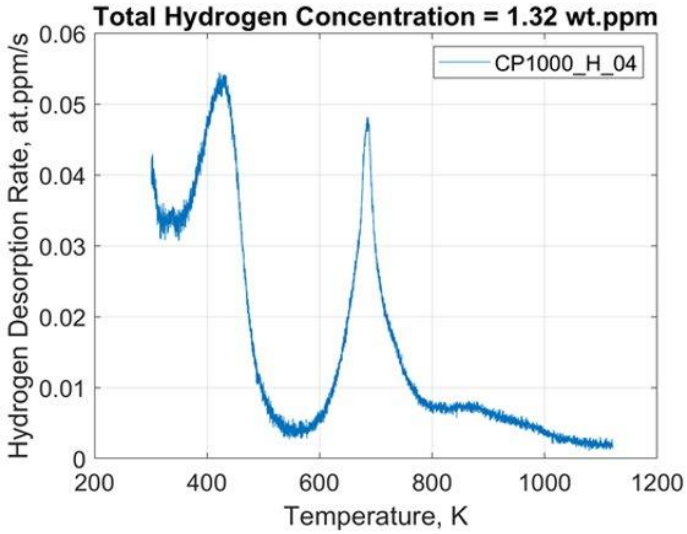

Figure 7: Hydrogen desorption rate vs. Temperature curve

Now, this curve must be used to calculate the total hydrogen concentration.

4.3.2 Methodology and Results

The formula to calculate the total hydrogen concentration is given by:

$$C_H = \left(\frac{1}{Heating\ rate}\right) * \int F\ dt \qquad (5)$$

Where F is the area under the hydrogen desorption rate (HDR) curve and the heating rate, as mentioned earlier, is 10 K / min. In the end, we represent the hydrogen concentration in wt.ppm unit.

Thus, we need to find the area of the HDR curve. For this purpose, MATLAB was used. Firstly, the HDR curve was fit with multiple Gaussian curves, which makes it easier to calculate the total area. So, the graph was divided at each minima of the HDR curve, and a Gaussian fit for each segment was found, as shown in Figure 8. Then, the area under each fitted Gaussian curve was calculated as an integral with the corresponding integral limits. The area under each curve was then summed up to finally obtain the total area. This value was divided by the heating rate according to the formula shown

earlier, which would finally give us the total hydrogen concentration in the sample. For the curve shown in Figure 8, we obtained the value for total hydrogen concentration as 1.2524 wt.ppm, after following this procedure.

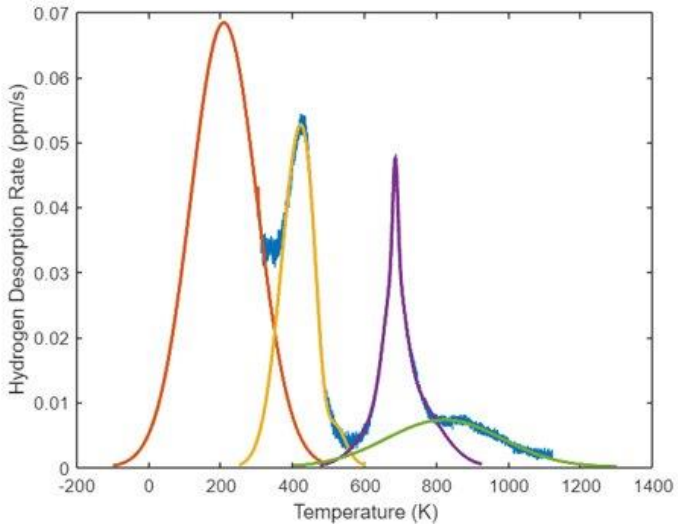

Figure 8: Fit Gaussian curves for the HDR curve

The Gaussian curves were fit using the MATLAB Curve Fitting toolbox. This allowed us to choose the degree of the curve, and gave us the optimized values of the coefficients of the curve equation, by minimizing the r-squared score. This toolbox provided the equations of the Gaussian curves, which could then easily be used to calculate the integral, by making use of the integral function in MATLAB. The resulting code is attached in the appendix.

The Gaussian equation containing two terms is as follows:

$$y = a_1 e^{-\left(\frac{(x-b_1)}{c_1}\right)} + a_2 e^{-\left(\frac{(x-b_2)}{c_2}\right)}$$

And the Gaussian equation containing three terms is as follows:

$$y = a_1 e^{-\left(\frac{(x-b_1)}{c_1}\right)} + a_2 e^{-\left(\frac{(x-b_2)}{c_2}\right)} + a_3 e^{-\left(\frac{(x-b_3)}{c_3}\right)}$$

In Figure 8, the red, yellow and green curves are Gaussian equations with two terms, while the purple curve is a Gaussian equation with three terms. The coefficients obtained for each of these curves are shown in Table 3.

Coefficients / Curve	Red	Yellow	Purple	Green
a_1	0.003055	0.05322	0.01685	0.007293
b_1	303.1	424.2	684.4	820.1
c_1	0.2219	77.36	9.945	226.3
a_2	0.06839	-0.01523	0.01846	-6.328e-05
b_2	207.9	484.3	682.1	808.1
c_2	129.7	33.53	39.41	3.278
a_3	-	-	0.01271	-
b_3	-	-	706.7	-
c_3	-	-	12	-

Table 3: Fitted coefficients for the Gaussian curves

This method can be improved. The Gaussian curves were not able to cover 100% of the area under the HDR curve, there are small gaps as seen in Figure 8. However, this method still gives us a reliable value for the total hydrogen concentration in the sample, which will be used as the initial value for the future MATLAB and Abaqus simulations to model the hydrogen diffusion.

Table 4 shows the total hydrogen concentration depending on the charging time for the specimens and Figure 9 shows the same information graphically.

Specimen	Charging Time (min)	Total H content (wt.ppm)
CP1000 H 05	60	0.43
CP1000 H 06	30	1.15
CP1000 H 07	10	0.80
CP1000 H 08	2	0.72

Table 4: Charging time vs. Total H content

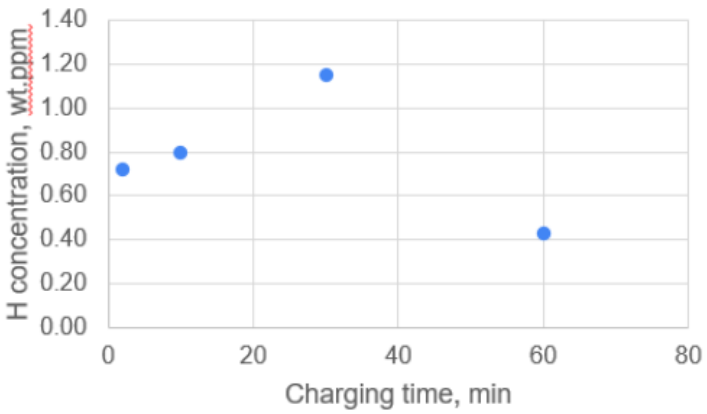

Figure 9: H concentration vs. pre-charging time

The primary conclusion from this data is that a charging time of 30 minutes will help reach the saturated state of hydrogen concentration in the sample. A drop of concentration with charging time of 60 minutes may be caused by local defects in the specimen.

4.4 Simulation: One-dimensional pure hydrogen diffusion using boundary condition method

When there is pollution in water bodies like streams or rivers with constant flow, the solution for the linear diffusion problem could provide useful insights by simulating the diffusion. Indeed, the solution for this particular situation is commonly utilized to solve similar problems, often as simplified versions of the problems in reality or simply when the information is only provided in only one dimension and still the beneficial result is required.

In this chapter, the Crank-Nicolson method, the key method used to solve the problem and to construct the algorithm to simulation will be introduced first. It will be solved in Abaqus first, and the simulation result will be presented. The construction and explanation of the algorithm in Matlab will follow next. The result in Matlab will also be presented with a comparison to the results from the simulation conducted using Abaqus.

4.4.1 Crank-Nicolson method for diffusion equation

This simple 1D diffusion problem was solved in Matlab using the Crank-Nicholson method [28], a finite difference method developed by John Crank and Phyllis Nicolson in the mid- 20th century for numerically solving the partial differential equations like heat equation. It is implicit and unconditionally stable for the diffusion equation. In the case where the thermal conductivity is much bigger than steps between the nodes backward Euler method can be used even though it is known to be less accurate in other situations because the Crank-Nicolson method might give less accurate results because of its oscillatory behaviors and backward Euler method is resistant and stable to oscillations.

The Crank-Nicolson method is based on the trapezoidal rule. It can be viewed as a mix of forward Euler and backward Euler methods. Let us solve our problem with the method. The traps were considered to be none for this simulation. The partial differential equation to be solved is the diffusion equation, where D is the diffusion constant.

$$\frac{\partial u}{\partial t} = D\frac{\partial^2 u}{\partial x^2} \qquad (6)$$

The Crank-Nicholson method discretizes the diffusion equation in the following form.

$$\frac{u_j^{l+1} - u_j^l}{\triangle t} = \frac{D}{2(\triangle x)^2}((u_{j+1}^l - 2u_j^l + u_{j-1}^l) + (u_{j+1}^{l+1} - 2u_j^{l+1} + u_{j-1}^{l+1})) \qquad (7)$$

With letting $\alpha = \frac{\triangle tD}{(\triangle x)^2}$, or applying a finite difference spatial discretization, and multiplying both sides by 2, the discretization can be written as below.

$$-\alpha u_{j+1}^{l+1} + 2(1+\alpha)u_j^{l+1} - \alpha u_j^{l+1} = \alpha u_{j+1}^l + 2(1-\alpha)u_j^l + \alpha u_{j-1}^l \qquad (8)$$

This is a matrix equation and can be written for the case of two interior points and two boundary points.

$$\begin{pmatrix} 1 & 0 & 0 & 0 \\ -\alpha & 2(1+\alpha) & -\alpha & 0 \\ 0 & -\alpha & 2(1+\alpha) & -\alpha \\ 0 & 0 & 0 & 1 \end{pmatrix} \begin{pmatrix} u_1^{l+1} \\ u_2^{l+1} \\ u_3^{l+1} \\ u_4^{l+1} \end{pmatrix} = \begin{pmatrix} 0 \\ \alpha u_1^l + 2(1-\alpha)u_2^l + \alpha u_3^l \\ \alpha u_2^l + 2(1-\alpha)u_3^l + \alpha u_4^l \\ 0 \end{pmatrix} \qquad (9)$$

The left hand side is triagonal and independent of time but the right hand side is dependent on time and needs to be updated before each time step.

4.4.2 One-dimensional diffusion problem solution conducted in Abaqus using the boundary condition method

The simulation was conducted using Abaqus 2020 installed in the Aalto student hub computer with a full license since the node size used is hundreds of thousands. The simple specimen geometries used in the modeling follow Figure 10. The thickness of the model used in the experiment is 1mm, however, in the Abaqus simulation, it was cut in half so that the simulation reflects a part of the simulation, from an outer surface to the center of the specimen so that the result can be shown logically.

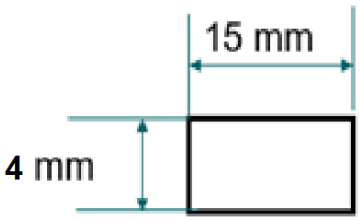

Figure 10: specimen geometries

The simulation was conducted applying uncoupled heat transfer analysis procedure in Abaqus. This is since the heat transfer analysis uses Fick's second law, which is similar to the diffusion equation as was mentioned in Section 3.3.1 and 3.3.2. Since the transient heat transfer analysis in Abaqus requires the definition of mass density, specific heat and conductivity, the equivalent values in our case must be found. As is shown by Barrera et al. [6], the diffusion and heat transfer equations are comparable and have analogous variables to one another. In the heat transfer equation, the degree of freedom is the temperature while in the diffusion it would be the hydrogen concentration [6]. Therefore, when defining the material in Abaqus, mass density and specific heat were set as 1, while conductivity, which would be analogous to diffusivity, was set as 3.07 * 10-4 mms^-2. Then a homogenous solid section was created with the just made material and assigned to the sample, after which an instance in the Assembly module is created as seen in Figure 11.

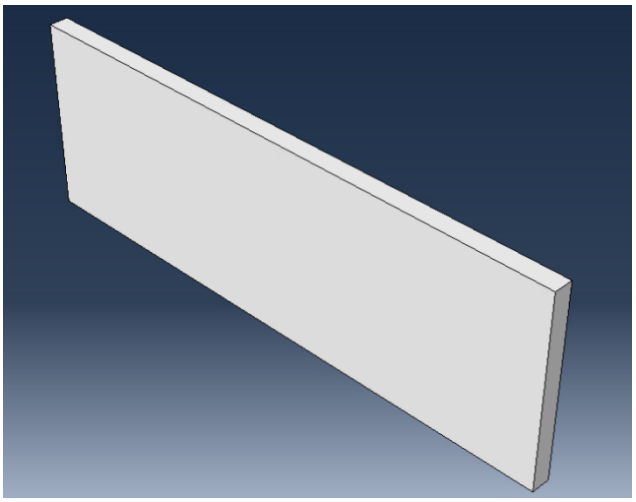

Figure 11: Assembly module created

In Step module, heat transfer was selected as the time step type. The time period for this simulation was set to be 2,000 seconds. Incrementation type was fixed, and the

maximum number of increments was 400. When the changes were less than 0.0001, the step was programmed to end so that the simulation skips the part where there are not enough meaningful values produced. The step module fields can be seen in Figure 12.

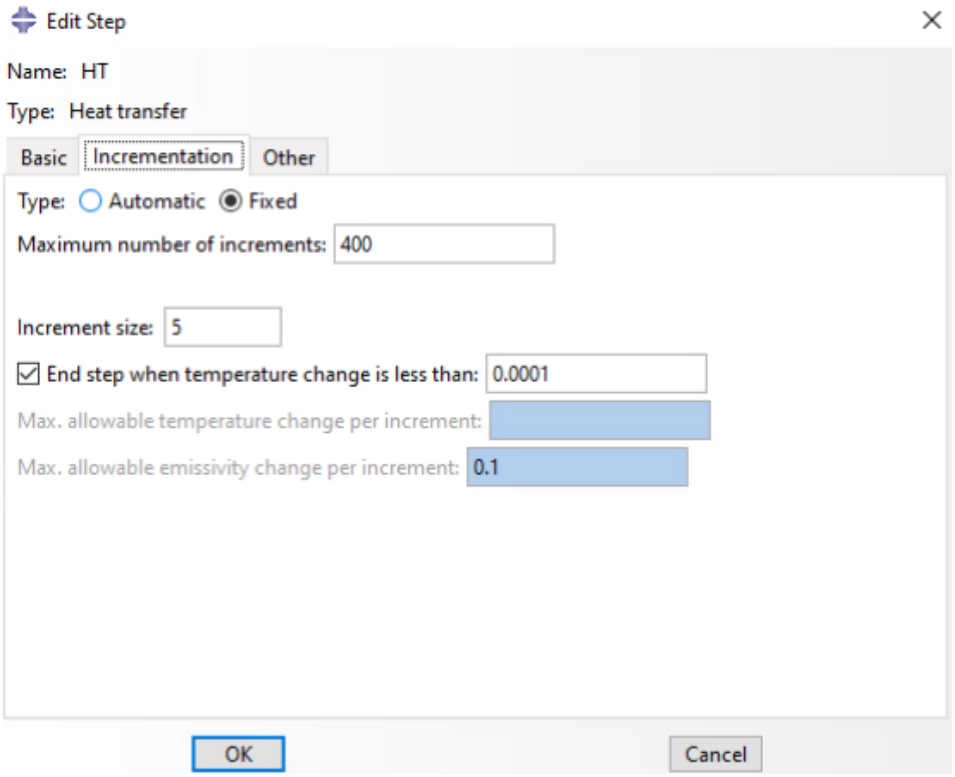

Figure 12: Step module fields

In Load module, two boundary conditions, one at zero and the other at 2.3 at.ppm were set on the red-colored side in Figure 13 and the opposing side, respectively. The magnitude of boundary condition was uniform on both sides. The boundary condition type was set to be temperature; however, this can be interpreted as hydrogen diffusion for our instance.

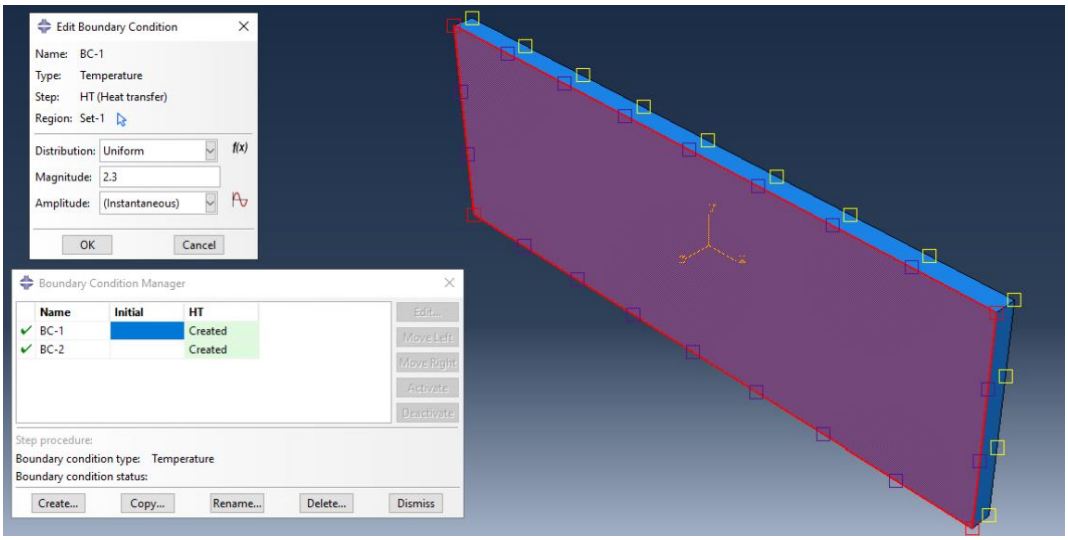

Figure 13: Load module fields, boundary condition applied on the other side as well with a magnitude of zero

In Mesh module, it is important to choose the element type of the part to be set as heat transfer. The approximate global mesh size is set to be 0.035, which creates approximately 900,000 elements, which will give smoother simulation results. The mesh size controls are shown in Figure 15. Along the thickness direction (z- axis), there are 15 nodes, which will correlate with Matlab simulation later on. The model was meshed after setting the variables. To be able to create a plot from the Abaqus results that can be then compared to the Matlab results, which is explained in more detail in the next section, a history output request was made. This was done by creating a new set under the Assembly tag as can be seen in Figure 14. The geometry that was selected was the surface along the thickness direction (z-axis). Then the history output request was created from the model tab. The domain was defined as set and the just created set was specified. From the output variables, nodal temperature (NT) was selected from the thermal tab, which in our case correlates to hydrogen concentration. This will allow us to see the hydrogen concentration at specific nodes. Once the history output request was created, the job file was created and submitted to finalize the simulation.

Once the job was finished, the data for the Matlab comparison was gathered. This was done by creating a path of nodes located along the thickness of the sample. In total 15 nodes were selected due to the mesh size as mentioned before. Then xy-data was created for the path that was just made. Every fifth increment was chosen to be plotted,

therefore the time step between each successive curve is 25s. The curves became linear when approximately 300s had elapsed, therefore 12 curves were plotted. This will be taken into consideration in the Matlab code as well. The xy-data from these plots was then exported to Excel by using the Abaqus provided plug-ins. The Excel file was then downloaded into Matlab and necessary code was written so that the data could be properly plotted alongside the Matlab results as will be seen in the next section.

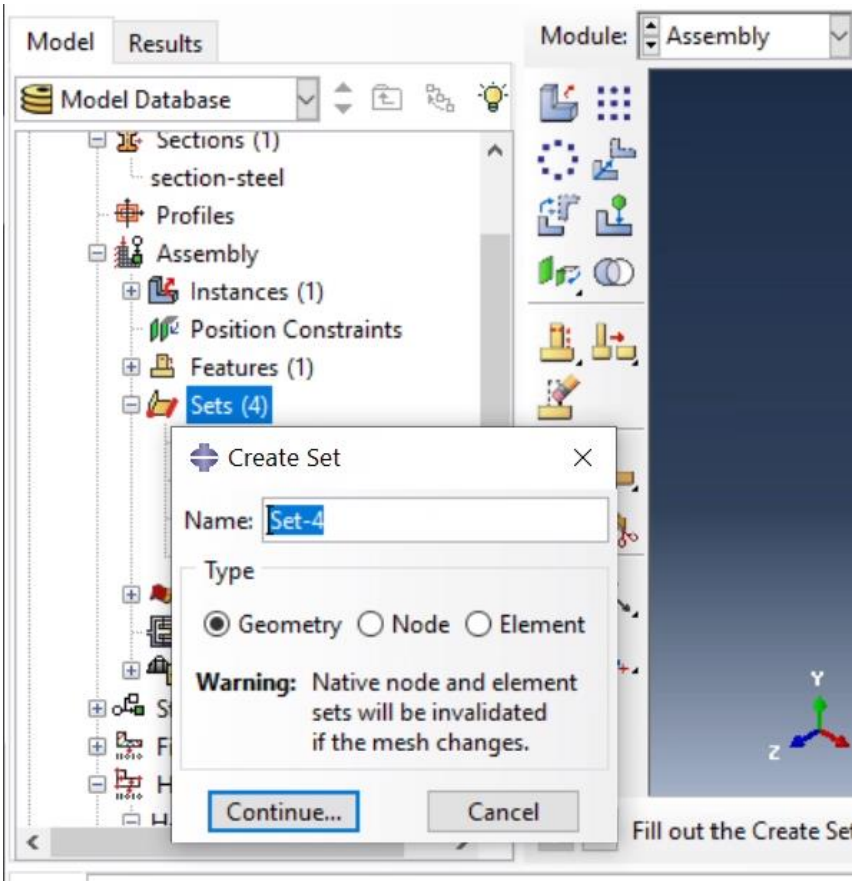

Figure 14: Creating a new set for the history output request.

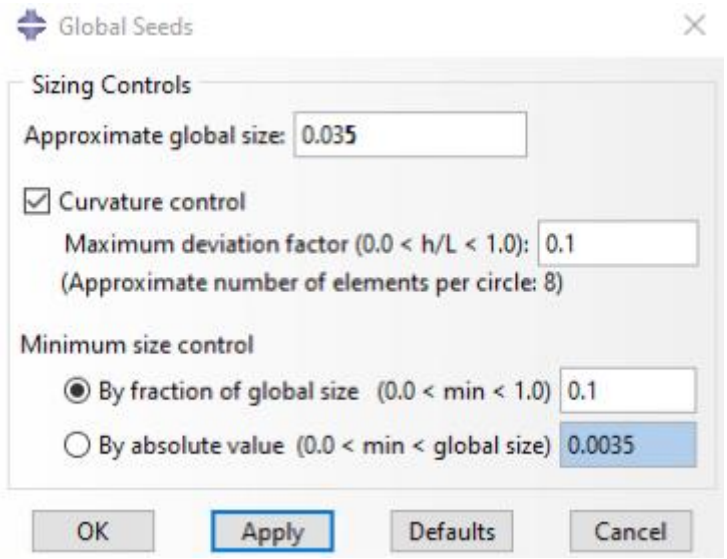

Figure 15: Mesh size controls

4.4.3 One-dimensional diffusion problem solution conducted in Matlab

The solution code for Matlab is outlined below.

1. Define domain, grid, and other necessary parameters.
2. Construct the time-independent matrix
3. Define the initial conditions for our case.
4. Enter a for loop that advances the solution.

4.1 Update the right-hand side of the matrix equation at the start of each time step.

4.2 Solve for u using the backslash operator.

4.3 Plot u versus x at fixed time intervals.

In our case, diffusion coefficient D was set to be 3.07*10^-4 mm^2/s. Defining x domain and x grid follows next. First, Lx is set to 0.5, since we would like the domain to be from 0 to 0.5. Nx sets the resolution or the number of spatial intervals. In our case, it is set to 14, which means 14 intervals on the x-axis. nx is the number of grid points or nodes on the x-axis, and it will equal one more than Nx, which will equal 15 in our simulation. dx is the grid length or spatial grid size in x. It will be Lx, the half of our domain length divided by Nx, the number of intervals. The x value of the grid is a vector. It is equal to starting from 0 to 0.5 since our total domain length is 0.5. Below is the snippet of the solution for defining the process.

```
D=3.07*10^-4; %diffusion coefficient mm^2/s

%%%%%%%% Define the x-domain and x-grid %%%%%%%%%%%%%%

Lx=0.5; %domain mm
```

```
Nx=14; % number of intervals
nx=Nx+1; % number of grid points in x, number of nodes
dx=Lx/Nx; % grid length in x
x=((0:Nx)*dx); % x values on the grid
```

Time step parameters are set next. Nsteps are the number of type steps. By defining nout as 5, the code outputs the solution every 5 time steps. A value for the time step dt is chosen as 5 for the solution. This is the borderline stability value for the forward time centered space scheme. Our equation has a parameter defined in, alpha defined to be dt times the diffusion constant divided by dx squared. So far, every parameter was assigned in a way they are not hardcoded so that they can be adjusted for later needs. Below is the code snippet for defining time step parameters.

```
%%%%%%%% Time step parameters %%%%%%%%%%%%%%%%%%%%%%%%
```

```
nsteps=60; % number of time steps
nout= 5; % plot every nout time steps
dt= 5; % borderline stability of Forward Time Centered Space scheme
alpha=dt*D/dx^2; % equation parameter
```

Next, the time-independent matrix is constructed. It has to be constructed only once. It is a banded matrix with three diagonals. Diagonals are defined first. The main diagonal, 2*(1 + alpha) along the main diagonal is multiplied by an nx-by-1 array of ones to make sure it has the vector of length nx. Two off diagonals are minus alpha multiplied with two columns of ones. Since this matrix contains many zeros, using sparse matrices can make the code more efficient. Therefore, the spdiags function, which is a function in Matlab that extracts nonzero diagonals and creates sparse band and diagonal matrices, was used in A. In A, one diagonal was put on the main, one below the main, and one above the main. It was specified that the matrix here is an nx by nx matrix. Then identity matrix was constructed using speye function, which returns a sparse nx by nx matrix for our solution. The boundary conditions are handled finally. Since this solution is for one-dimensional problem, there are only two boundary points. The matrix A constructed earlier is modified so that the first and the last rows are replaced by the identity matrix in the sparse representation from before. This sets up the boundaries in matrix A. The code for this part is below.

```
%%%%%%%% Construct the matrix %%%%%%%%%%%%%%%%%%%%
```

```
diagonals=[2*(1+alpha)*ones(nx,1), -alpha*ones(nx,2)];
```

```
A=spdiags(diagonals,[0 -1 1], nx, nx);
I=speye(nx);
A ([1 nx],:) = I([1 nx],:);
```

Next, initial conditions are defined. In our particular case, u is firstly set to be an 1-by-nx sized array of zeros, with the first element of 1 considering the given initial condition. After taking the transpose of u so that it becomes a column vector, it is set. Below is the code snippet for this part.

```
%%%%%%%% Define initial conditions %%%%%%%%%%%%%%%%%
u=zeros(1,nx);
u(1)=1;
u=u';
```

Finally, we get to the computational engine of the code, also graphics and the plotting routine is set up here so that the results can be plotted visually.
By constructing the right-hand sides and solving it, the diffusion equation is developed. The solution is time advanced, also it is plotted every nout time steps at the same time. For loop is constructed from 1 to nsteps, which is the total number of time steps that we are revolving the diffusion equation. Right-hand side is constructed because it is dependent on time as it depends on the solution itself. When setting matrix b, two endpoints are set as the initial input value 2.3 and 0 respectively according to our initial boundary condition. Now that the right-hand side for the Crank-Nicolson method is implemented, we can solve the Crank-Nicolson method at each time step using the backslash operator. This process takes the most time in the calculation, however, it is still a very fast computation because matrix A is a sparse matrix with three diagonal sparse matrices. Alternatively, LU decomposition of matrix a can be conducted so that running code would take slightly less time, however current computation runs fast enough for our solution. Then x and u are plotted.

Every time the index number for the for loop, m, passes nout times, another curve is added to the plot. To compare the results gained from Matlab with the results from Abaqus, the file containing results from Abaqus is read and plotted on the same plot. The blue curves indicate that the curves are results of Matlab calculation and the red

curves indicate Abaqus calculation results. Below is the code for the final part and the plotted outcome.

```
%%%%%%%% Advanced solution and plot %%%%%%%%%%%%%%%%%

for m=1:nsteps
b=[2.3;[alpha*u(1:nx-2)+2*(1-alpha)*u(2:nx-1)+alpha*u(3:nx)]; 0];
u=A\b;
if mod(m,nout)==0, plot(x,u,'b');hold on, end % blue is for matlab
end

T = readmatrix('matlab_5.xlsx');

[m,n] = size(T);
xlabel('Thickness direction (z-axis),mm');
ylabel('Hydrogen concentration, at.ppm');

for t = 1:(n/2)-3
plot(T(:,t+(t-1)), T(:,t+t), 'r');hold on; % red is for abaqus
End
```

4.4.4 One-dimensional diffusion problem solution conducted in Abaqus using flux load method

Alongside the boundary condition method, the flux load method was also implemented. The main reason for the implementation of the flux load method was to provide a more accurate presentation of the experimental scenario. The flux load method mainly followed the same methodology as the one-dimensional boundary condition method, which is described in section 4.4.2. The only differences in methodology are in the Step and Load modules, which will be described below.

In the Step module, two steps are created instead of one. The first step is the flux load step, which introduces hydrogen into the sample. The time period is 1920 seconds with automatic incrementation, where the maximum increment number is 38 and increment size is initially 50, minimum 0.0192, and maximum 500. Also, a condition is set that the step will end when hydrogen concentration change (temperature change in Abaqus) is less than 0.0001. Moreover, the maximum allowable temperature and emissivity change per increment parameters are set to 1000 and 0.1 respectively. The second step, which is the step when the entered hydrogen diffuses in the sample to a uniform concentration, has time period of 2000 seconds and automatic incrementation. The maximum number of increments is 100000, where the initial increment size is 10,

minimum 0.02, and maximum 400. Again, a condition for the minimum hydrogen concentration change is set at 1*10^-7. The maximum allowable temperature and emissivity change per increment parameters have values 1000 and 0.1 respectively.

In the Load module, instead of a boundary condition, a load of type surface heat flux with the flux step was created. The flux was set on only one of the surfaces as can be seen in Figure 16 and the magnitude was set as 0.0003 at.ppm/(mm^2*s), which was derived by the following method:

0.0003 at.ppm/(mm^2*s) * [surface area] 60 mm^2 * [timesteps] 1920 = 34.56 at.ppm

Since we halved the width of the sample when simulating, 34.56 at.ppm is only half of the whole concentration. Therefore, we must multiply the value by 2 to get the total hydrogen concentration:

34.56 at.ppm * 2 = 69.12 at.ppm

This value must then be divided by 60 atomic weight units so that units are converted to wt.ppm and therefore get the value calculated from the TDS measurement for the total hydrogen concentration:

69.12 at.ppm / 60 = 1.15 wt.ppm

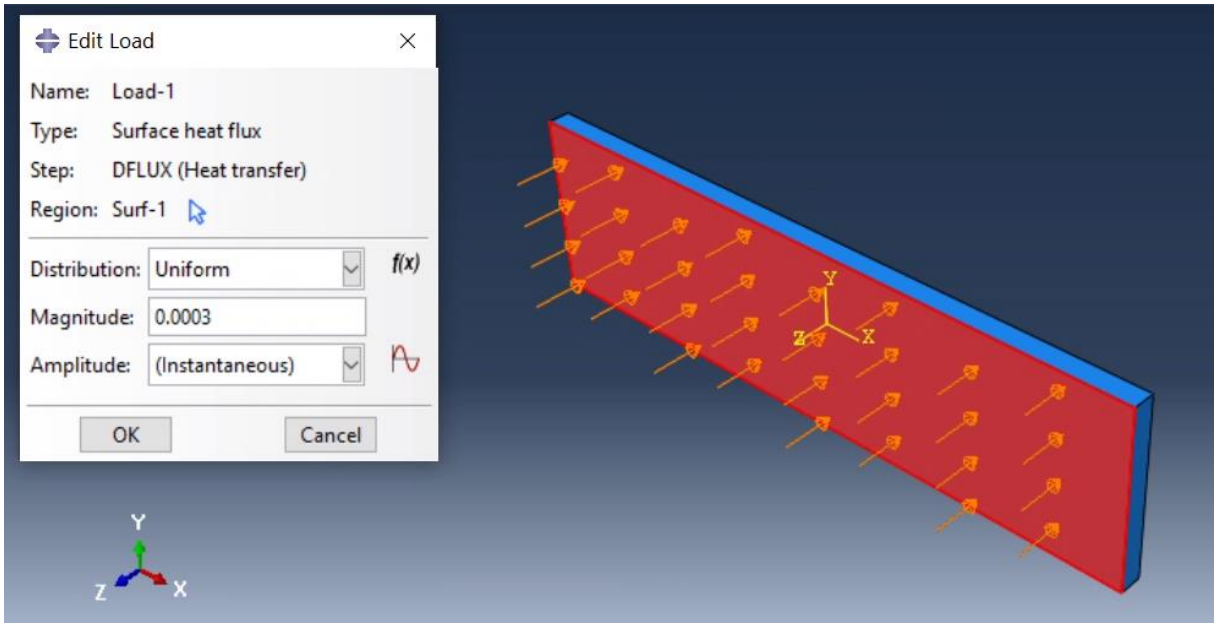

Figure 16: The flux load that was created in the one-dimensional case.

4.5 Simulation: Three-dimensional pure hydrogen diffusion using boundary condition method

To simulate pure hydrogen diffusivity in samples of varying geometry, Abaqus 2020 by Dassault Systèmes was used. The main goal of this simulation was to replicate the way hydrogen diffused into the samples. It is essential that the license is not a student one, which limits the node amount to only 1,000. The simulations were conducted on the Aalto computers located in the Student Hub, since they had a full Abaqus license. The different specimen geometries used in the simulations are shown in the Figures below. In Figure 10, the simplest geometry can be seen, which is just a 4x15 mm rectangle. The notched geometry, which is shown in Figure 17, had four different notch sizes (2.5, 6, 15 and 40 mm). The central hole geometry also had two different sized holes, 2- and 4-mm diameter. An example of the latter is shown in Figure 18. The most complex geometry is shown in Figure 19; a more detailed view into the dimensions of the specimen is also shown in the same Figure. All specimens had a width of 1 mm. Each of these four different geometries were modeled and recreated in Abaqus in the Parts module. Due to symmetry, only a quarter of the simple, central hole and notched geometry specimens was modeled. An example is shown in Figure 20 with the 15 mm notched sample. Moreover, the width of the samples in Abaqus was set as 0.5 mm so that diffusion could be studied more clearly, and any unnecessary computation could be avoided.

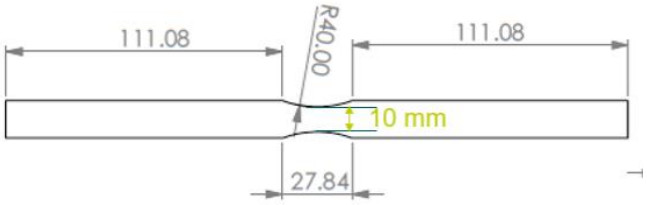

Figure 17: Notched geometry

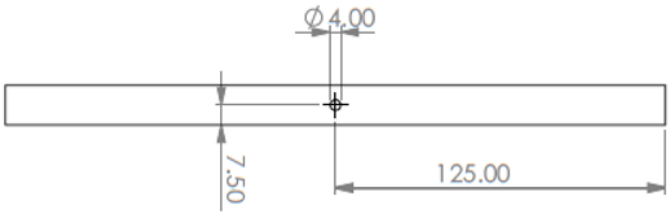

Figure 18: Central hole geometry

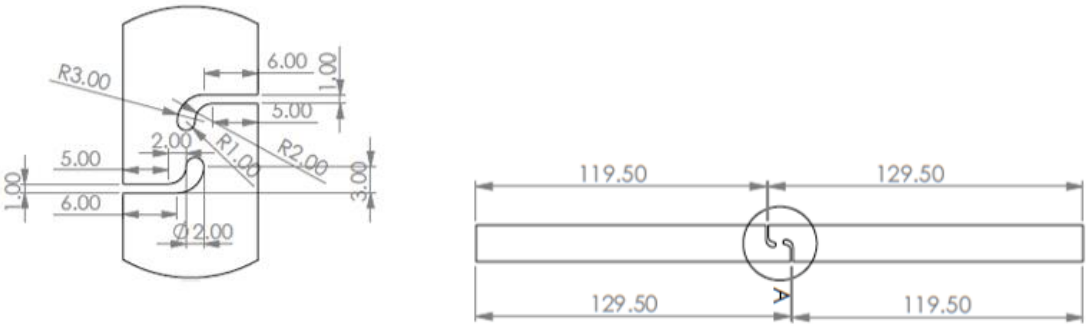

Figure 19: Complex geometry

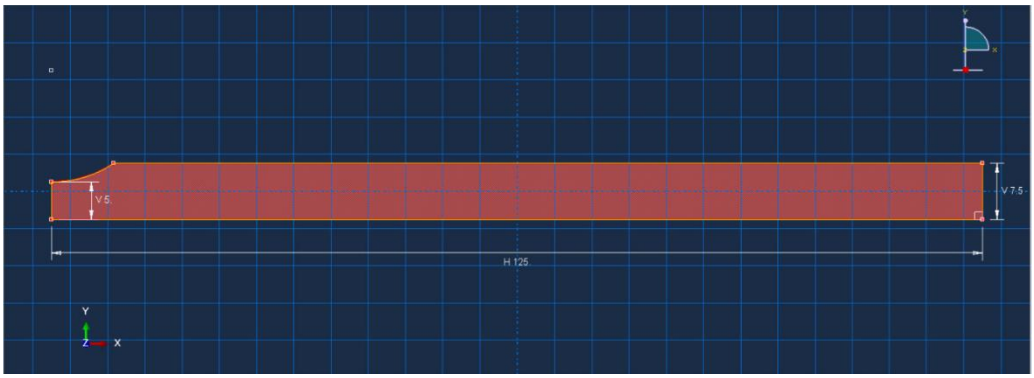

Figure 20: Example of 15 mm notched sample.

These simulations were conducted using Abaqus' heat transfer analysis method, like in the one-dimensional analysis case. The same values that were used in the one-dimensional case for the specific heat, mass density, and conductivity were specified in the Property module for the three-dimensional cases. Then as in the one-dimensional case, a homogenous solid section was created with the defined material and assigned to the sample, after which an instance is created in the Assembly module.

When creating the time step in the Step module, the type was selected as heat transfer. The time period for each simulation was kept the same at 100,000 seconds, with increment type being fixed with the increment size and the maximum number of increments being 10 and 10,000 respectively. However, due to the large time period, a condition was specified that once temperature change, in our case hydrogen concentration change, is less than 0.0001 the step ends so to keep the run time of the simulation manageable.

In the Load module, boundary conditions were set for specific surfaces of the sample. In this case, the boundary condition type was set to Temperature, which would variable-wise correlate to the hydrogen concentration. It is important to remember that the modeled sample is only a quarter of the actual size therefore the outer surfaces of the sample have to be determined carefully so that the boundary conditions are only set on the outer surfaces of the whole sample. Once the correct surfaces were selected, the boundary value is set to 1.15 at.ppm. This value is the hydrogen concentration.

Before choosing the mesh size, the element type of the part has to be specified in the Mesh module. Since the method used is heat transfer the element type would also be of this type, therefore heat transfer is chosen from the family section and otherwise, the inputs are left the same. When making the mesh, the approximate global size used for all the samples was set to 0.1, since this provided a detailed enough mesh to study. The part has then meshed, and a job was created in the Job module and submitted.

4.6 Simulation: Three-dimensional pure hydrogen diffusion using the flux method

The flux method was used to improve the accuracy of the three-dimensional pure diffusion problem to the real experimental scenario. The complex geometries that were introduced in section 4.5 were used in the simulations so that the flux and boundary methods could be compared in the results and discussion section. Moreover, the flux method follows the same procedure as the boundary in the Part, Property, Assembly, Mesh, and Job module. The differences in methods are found in the Step and Load modules.

In the Step module, rather than creating only one step, two steps are made. The first step is the flux step, during which the hydrogen enters the sample at a rate that will be defined in the Load module later. The time period for this step is set at 1920 seconds, with a fixed incrementation type. The maximum increments are 32 with an increment size of 60. A condition is set to end the step when the change in hydrogen concentration is less than 0.0001. The second step that was created is the diffusion step, which is when the hydrogen that entered the sample diffuses through the

sample to reach a uniform concentration. The time period for this step was set to 5000 seconds and the fixed increments were of size 50 and a maximum number of 100 increments. A similar condition was set during this step as in the flux step.

In the Load module, the flux loads have to be set to the flux time step. A surface heat flux load was created with the magnitude of 0.0003 at.ppm/(mm^2*s), which is the same value that was used in the one-dimensional flux case. As has been explained in earlier sections, the heat flux would be analogous to the hydrogen flux. This flux was applied to the same surfaces as the boundary conditions were applied to in the boundary condition method. No boundary conditions or flux loads were set for the diffusion step.

5. Results and discussion

5.1 Simulation: One-dimensional pure hydrogen diffusion

One-dimensional pure hydrogen diffusion was done to verify that the methods used are reliable and portray the actual experimental scenario to some degree. Ultimately, two different methods were used to show the diffusion problem – boundary condition and flux load method.

5.1.1 Results: Matlab and Abaqus boundary condition

In section 4.4.3, the Matlab code shown plots both the Abaqus hydrogen diffusion results and the results derived by using the Crank-Nicolson method. The final plot can be seen in Figure 21. The x-axis shows the change along the thickness of the sample in mm, while the y-axis corresponds to the changes in hydrogen concentration with units at.ppm. The Matlab results are in blue, while the Abaqus are in red. Time increases diagonally as is shown with the arrow, therefore as time goes on, both Abaqus and Matlab results become more and more linear. The lines become completely linear at total time of 300s and the time step between curves is 25s. At 300s, the results of the Abaqus simulation can be seen in Figure 22, which shows a completely linear distribution of hydrogen along the sample's thickness. The results overlap in each time step; the most deviation can be seen in the first time step at 25s, however even then the deviation is quite small.

5.1.2 Discussion: Matlab and Abaqus boundary condition

The resulting graph shows the rate of diffusion, and the reliability of the heat transfer method used in Abaqus. Hydrogen concentration changes with each time step as is shown in Figure 21. The Figure shows that the diffusion happens at a faster rate at the start of simulation, and then slowly reaches an equilibrium. These methods can be applied to solving similar diffusion problems in real-life scenarios where data is given in only one dimension or in a simplified version of scenario to identify the diffusion rate and profile according to geometry and other parameters. The most important fact that the Figure shows is the overlap between the Matlab and Abaqus data. The graph shows that the heat transfer analysis method used in Abaqus provides accurate results

to the hydrogen diffusion problem due to the significant overlap in the results. The method using Matlab validates the Abaqus method, vice versa. However, the boundary condition does not well represent real-life experiment situation as the method is too simple and idealistic. This is due to the fact that the boundary condition sets on surfaces at maximum hydrogen concentration at all times, which does not represent the actual experimental scenario. In reality, the hydrogen concentration should change with time as hydrogen is distributed into the sample. Therefore, the flux method was proposed to consider the more complex nature of hydrogen diffusion as was discussed earlier in section 4.4.4.

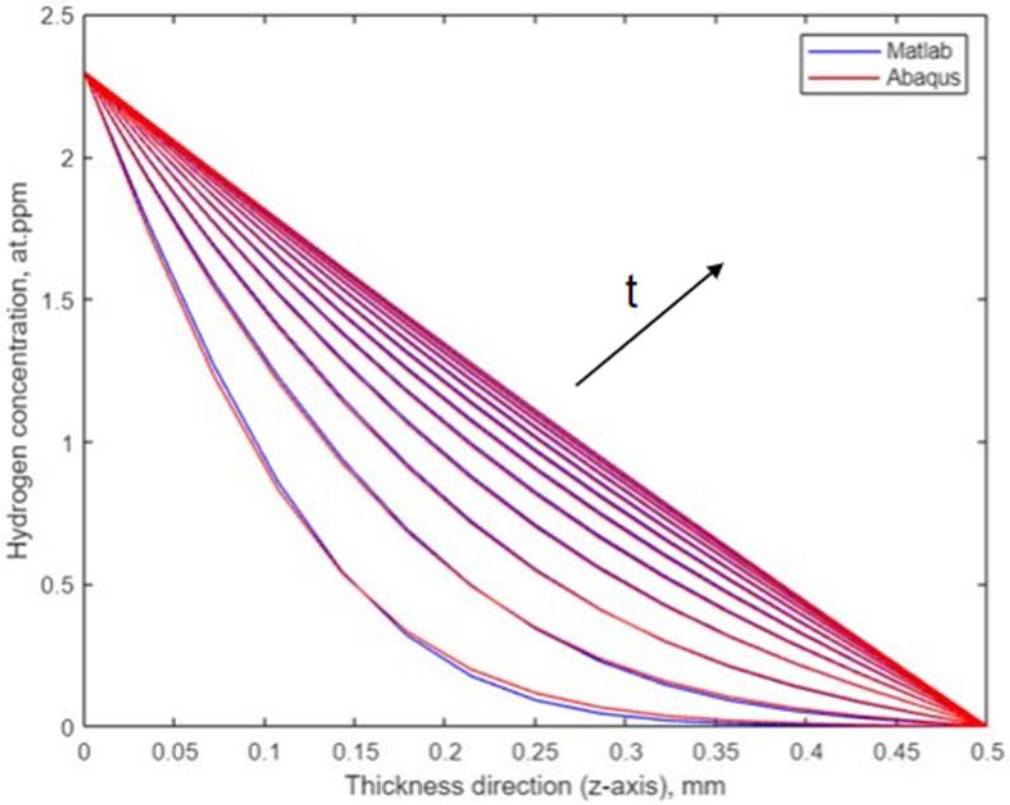

Figure 21: The results of the one-dimensional Matlab and Abaqus boundary methods.

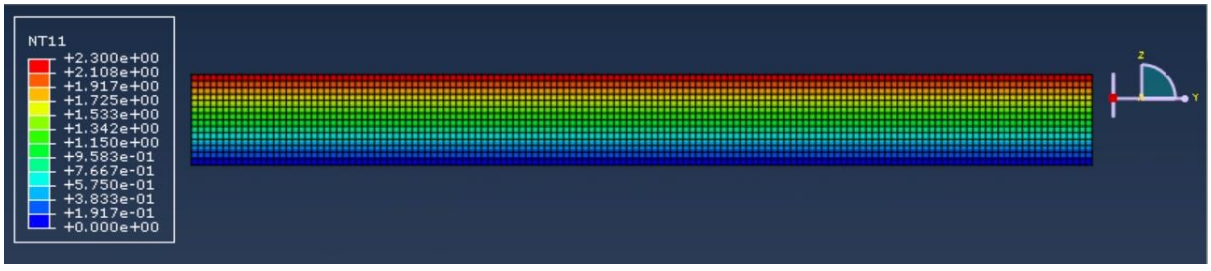

Figure 22: Abaqus simulation at 300s.

5.1.3 Results: Abaqus flux load method

The flux load method in section 4.4.4 was used to show a more accurate outcome to the actual experimental scenario. The results of this method are shown in Figures 23 and 24. Figure 23 shows the diffusion step, when the hydrogen diffuses into the sample after the flux step has been completed. As can be seen in Figure 23, the hydrogen concentration decreases with time. The initial condition at the start of the diffusion step is shown by the red curve and as time goes on the curves begin to level out till they become completely horizontal. The final result is shown by the yellow curve, which is completely horizontal at about 1.15 at.ppm/mm^3 when the step time is 1450s. Figure 24 shows the progression of hydrogen diffusion through the width of the sample during the flux and diffusion steps till a uniform concentration of hydrogen throughout the sample is reached. The flux is positioned on the left surface of the sample. Hydrogen concentration reaches an all maximum at the flux surface when flux step reaches its end so approximately between 1850-1920 s. The diffusion step results are shown in the very last subfigure of Figure 24, which has a uniform orange color.

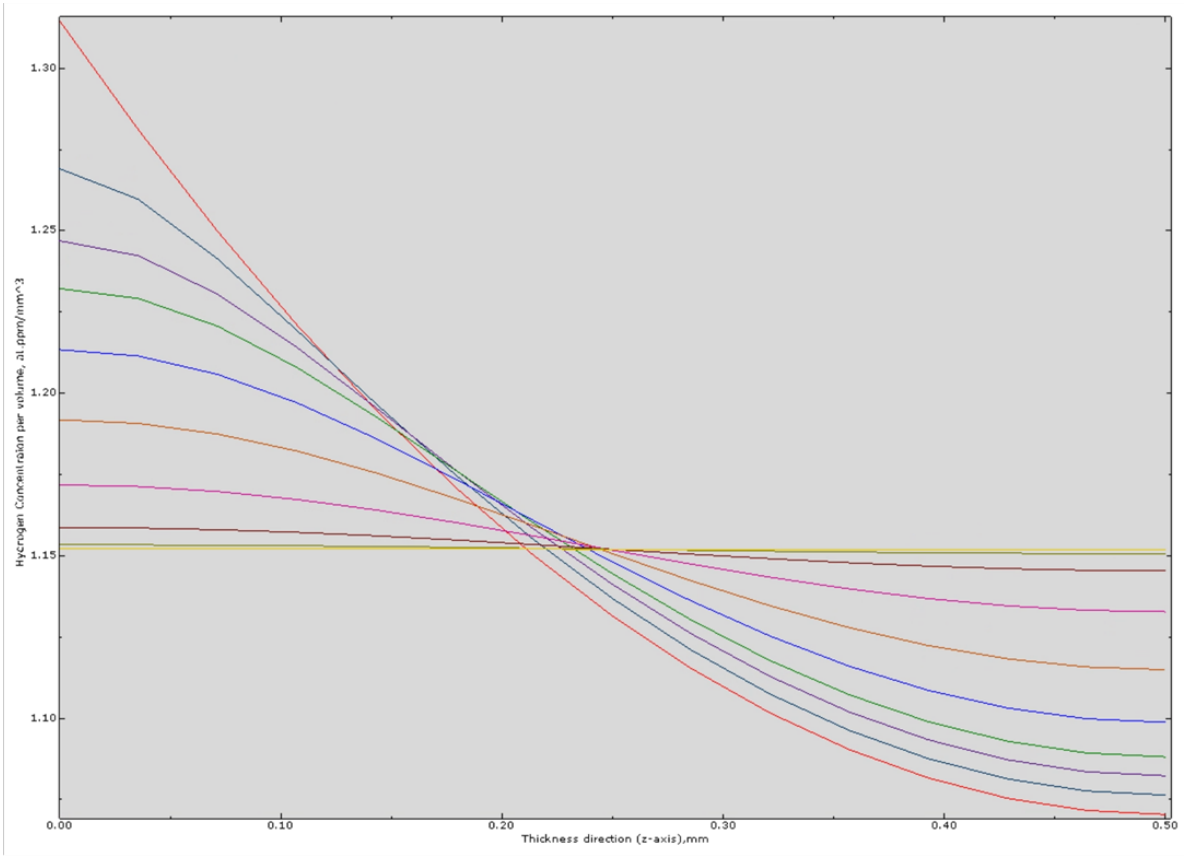

Figure 23: Diffusion step during which hydrogen diffuses into the sample.

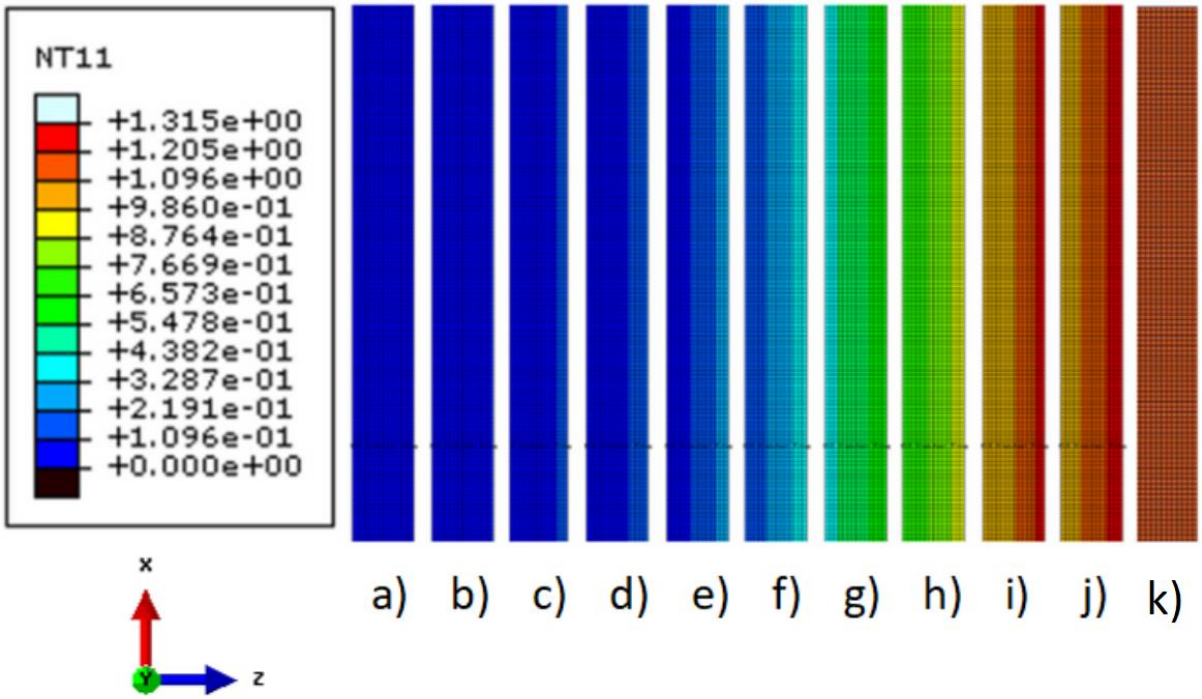

Figure 24: The Abaqus simulation results at a) 0s b) 50s c) 100s d) 150s e) 250s f) 450s g) 850s h) 1350s i) 1850s j) 1920s k) 2090s

5.1.4 Discussion: Abaqus flux load method

The main difference between the boundary condition and flux method is that the flux method does not require any set boundary conditions, therefore allowing the simulation to be more realistic. As mentioned in section 5.2.2, the boundary condition simplifies the phenomenon of hydrogen diffusion to a greater extent than the flux, which reduces the accuracy and complexity of the boundary condition method result. By setting two steps, one for flux and the other for diffusion, this allows for uniform hydrogen concentration to be reached during the simulation as is shown in the last section's Figures, which correlates more with the actual experimental scenario. However, for the flux method to be exact, TDS tests must be done on a pre-charged sample of specific geometry so that total hydrogen concentration values are known, and the appropriate flux parameters are used in the simulation.

5.2 Simulation: Three-dimensional pure hydrogen diffusion

The simulations were conducted using two different methods on each presented geometries as in section 4.5. Both methods, pure hydrogen diffusion using boundary condition and flux load method were explained in detail in the previous sections. The results from the simulations will be presented according to the different geometries, allowing comparing the differences coming from the two methods more easily.

Before the visualized results according to geometries are presented, detailed overall performance is studied by using the Figures below. The outcomes vary for the boundary condition method and heat flux method. The model used for producing these results was the 15 mm notched dog bone model, however these graphs show the general behavior of the three-dimensional flux load method during the flux and diffusion steps, which were simulated for each complex geometry.

Figure 25 shows hydrogen concentration level along the thickness direction as it changes during the total time of 1920s. The legend indicates the time step lines in order from top to bottom. For simplicity, a curve was plotted every 60s so the red curve would be at time zero and the next curve at time 60s and so on. Each step appears to be similar in terms of shape, however on different hydrogen concentration levels. This shows that the hydrogen is diffused in a similar manner throughout the simulation until the final stage is reached in the flux step.

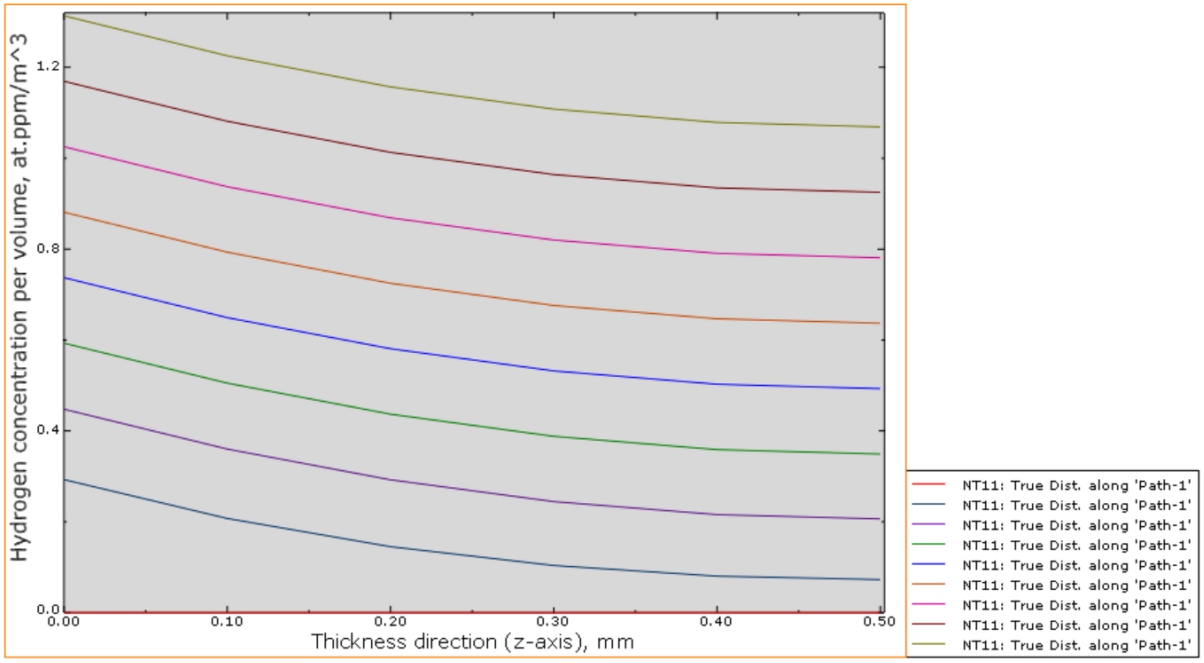

Figure 25: Flux step pattern where time step between curves is 60s and intial time 0s.

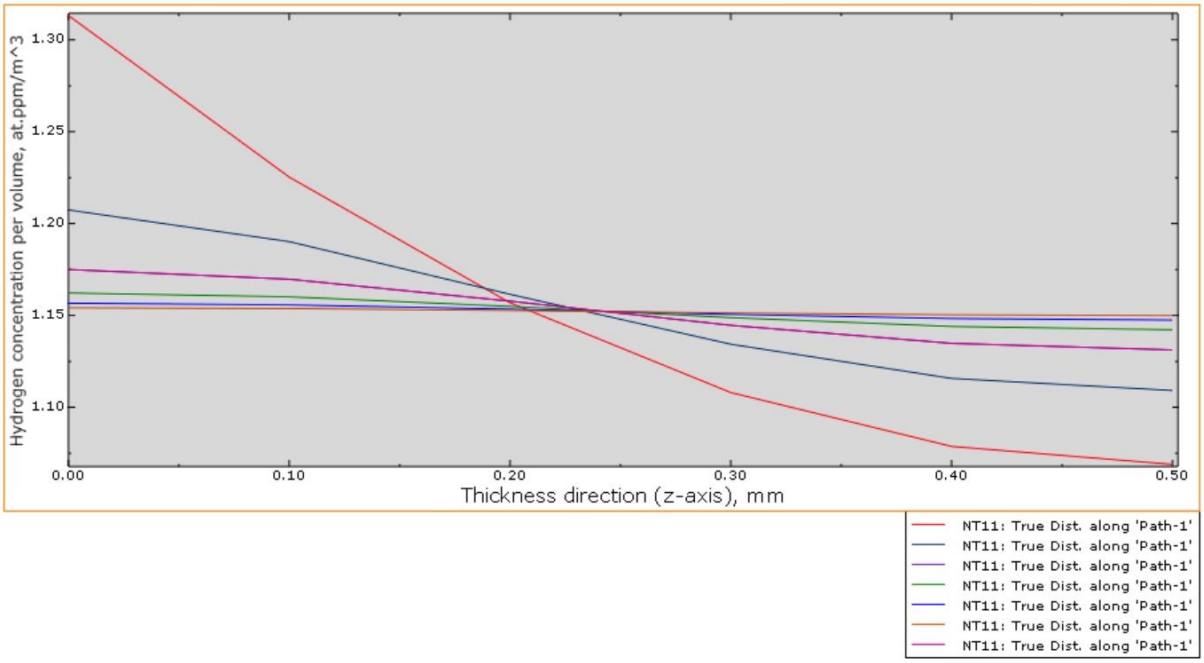

Figure 26: Diffusion step pattern, where time step between curves is 100s and final time is 2420s.

In Figure 26, the first six time steps of the diffusion step were plotted, since they showed the most visible differences. The rest of the time steps exhibited similar outcome of evenly distributed hydrogen along the thickness. The first curve, which is

in red, shows the result of the flux step. The time step between the curves is 100s, therefore the last and most horizontal curve shown in the Figure would have been at total time 2420s.

5.2.1 Results: Notched dog bone

The first three-dimensional simulation is conducted on a model of notched dog bone with 15mm radius geometry. Figures will be shown in a manner that describes the hydrogen concentration distribution for certain time steps. In the left top part of the Figures, a legend describing hydrogen concentration level being mapped into different colors can be found. The viewport is given as axis below the legend.

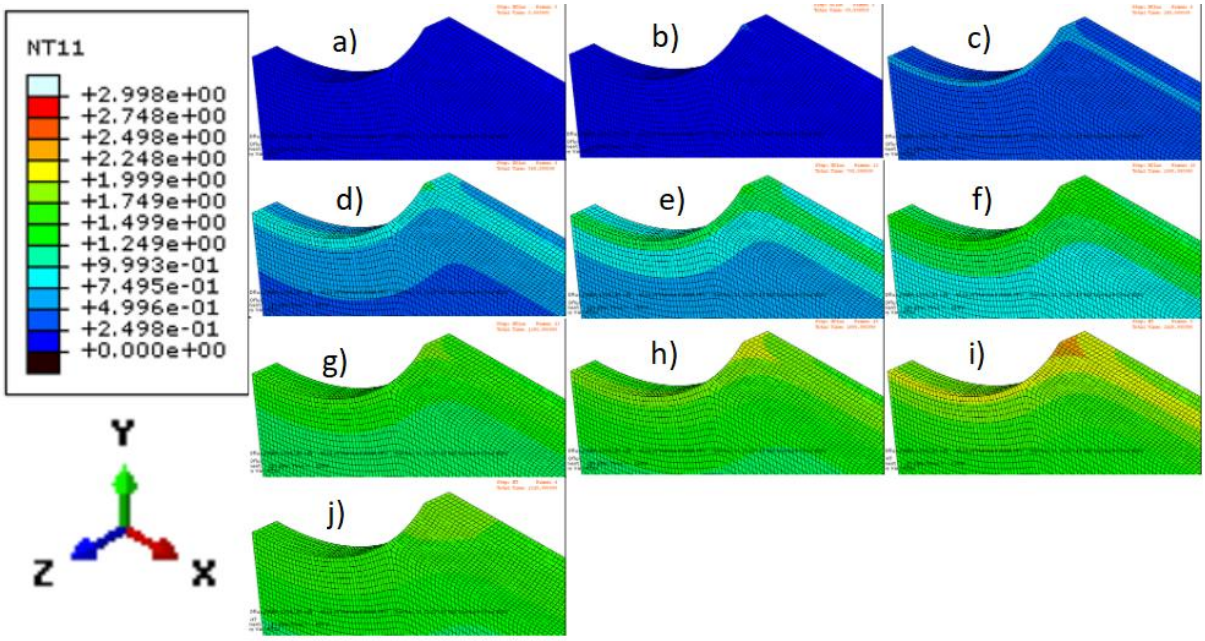

Figure 27: Flux method results for 6mm notched dog bone at a) 0s b) 60s c) 240s d) 540s e) 780s f) 1080s g) 1380s h) 1680 i) 1920s j) 2320s

Figure 27 shows the results for the 6mm notched dog bone sample. A flux load of 0.0003 at.ppm/(mm^2*s) is applied to the surfaces seen in the Subfigures from a) to h), therefore they are in the flux step. Subfigure i) is the first frame of step therefore it shows the results of the flux step. There is a higher concentration of hydrogen at the corner of the sample and along the edges throughout the flux step. The hydrogen

diffuses into the sample from the high concentrations at the edges and corners. In j) (at 2320s), the hydrogen has uniformly diffused in the sample.

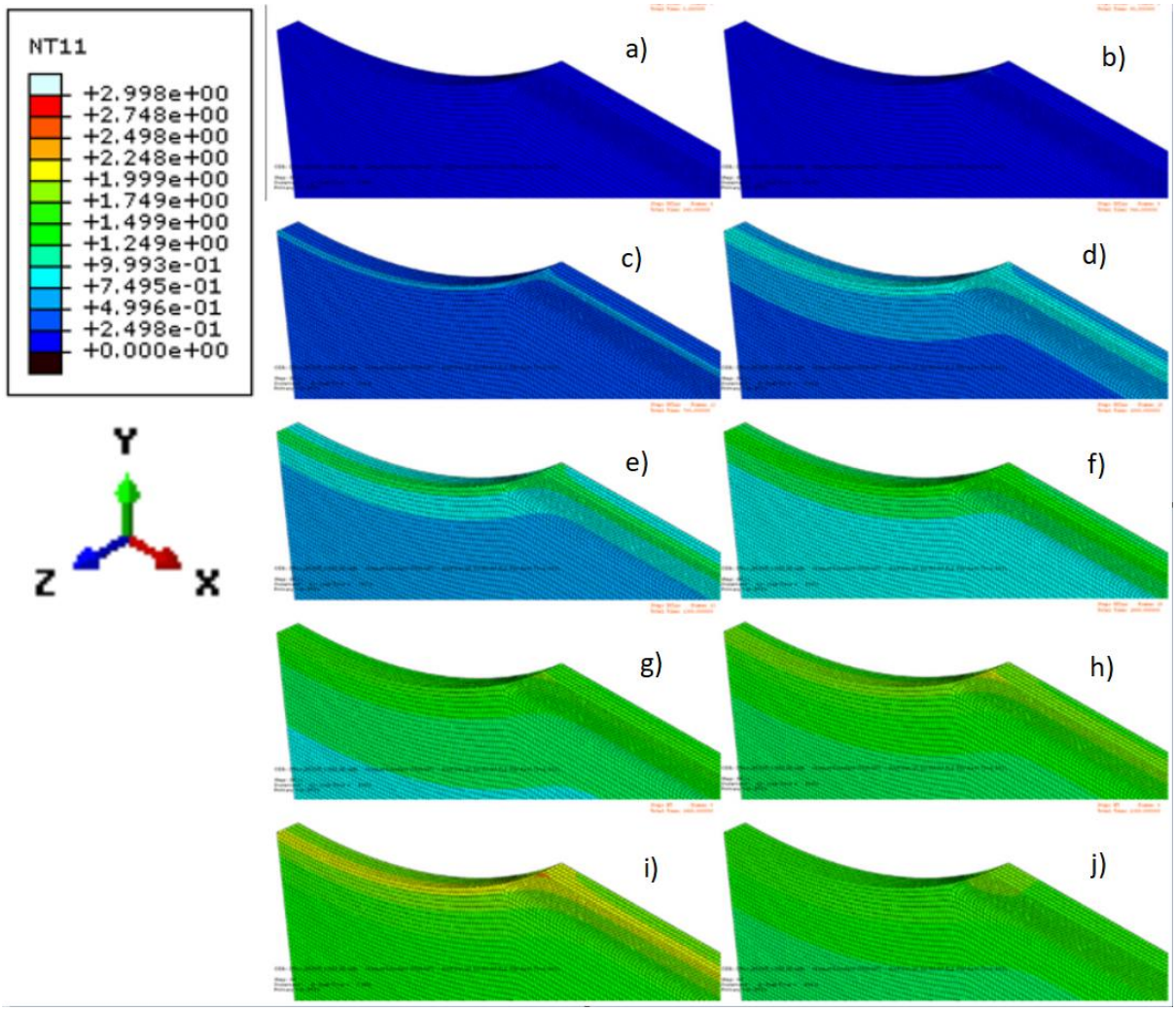

Figure 28: Flux method results for the 15 mm notched dog bone sample at a) 0s b) 60s c) 240s d) 540s e) 780s f) 1080s g) 1380s h) 1680 i) 1920s j) 2320s

Figure 28 shows the flux method results for the 15 mm notched dog bone sample. The flux step is shown in Subfigures from a) to h) and the diffusion step from i)-j). As with the 6mm notched dog bone sample the edges and corner show the highest concentration of hydrogen.

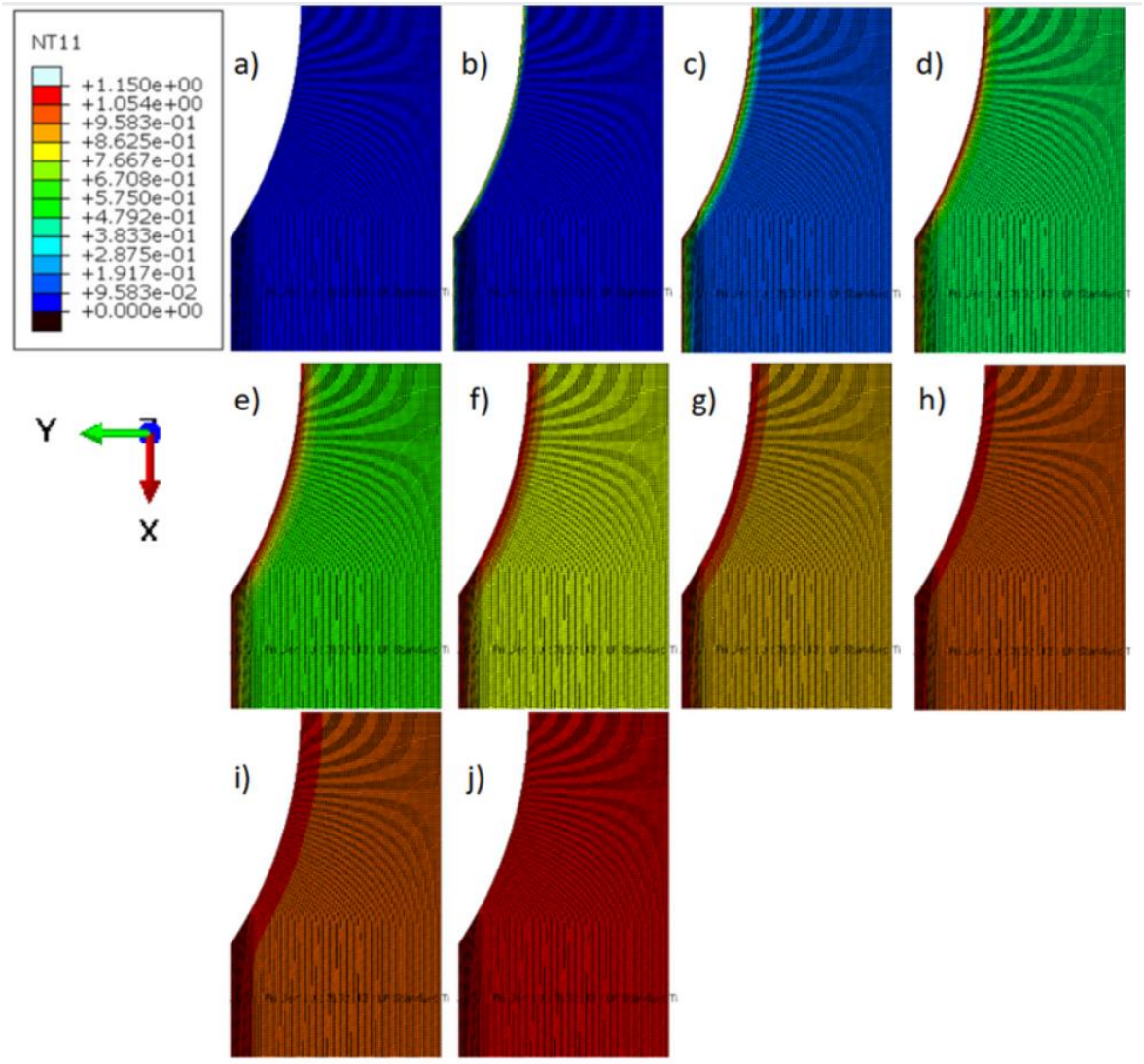

Figure 29: Boundary condition results for the 15 mm notched dog bone sample a) 0s b) 10s c) 100s d) 220s e) 340s f) 460s g) 580s h) 700s i) 820s j) 940s

Figure 29 shows the simulation result of hydrogen diffusion using hydrogen boundary condition method. As the Figure illustrates, diffusion started from the outer surface slowly and continued with a faster speed until it reached to a close level of evenly distributed hydrogen at the final stage shown in Subfigure j), which would be at time 940s.

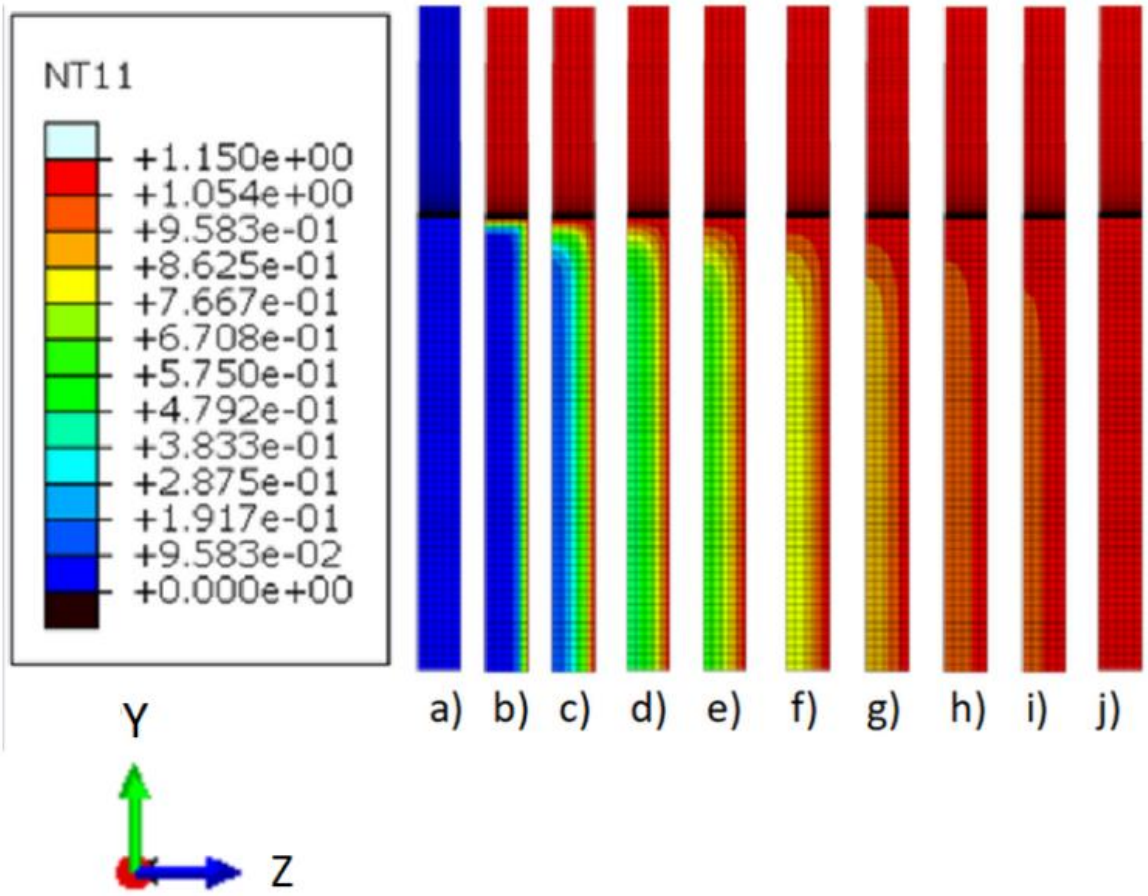

Figure 30: Profile view of 15 mm notched dog bone model with boundary condition applied at a) 0s b) 10s c) 100s d) 220s e) 340s f) 460s g) 580s h) 700s i) 820s j) 940s

Figure 30 shows the same simulation from the angle of the side with the notch. The boundary condition of higher hydrogen concentration applied on the right side and the notched part is shown from Subfigure b) onwards in the Figure. It can be confirmed the rectangular part of the model is affected from the outer surface to inside until even distribution of hydrogen concentration is reached at time 940s.

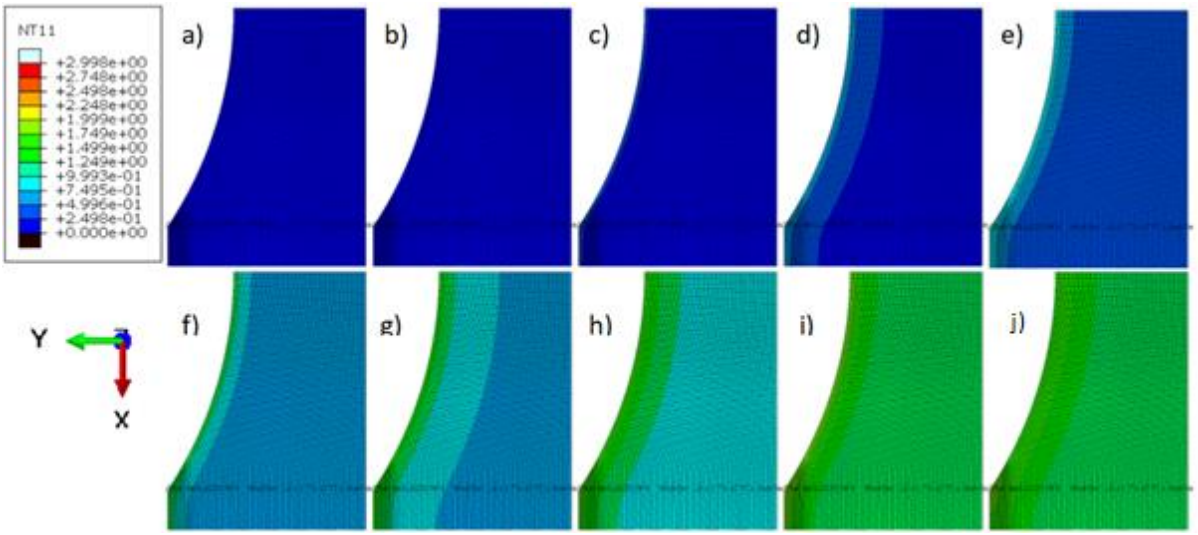

Figure 31: Flux load method results for 15 mm notched dog bone model at a) 0s b) 180s c) 240s d) 540s e) 720s f) 1020s g) 1380s h) 1740s i) 1920s j) 2820s

Figure 31 shows the flux load results for the 15 mm notched dog bone from a different viewpoint. The flux step is shown in Subfigures a) to i) and diffusion step is shown in Subfigure j). The Figure does not seem to exhibit much difference, except that the values are mapped with different colors now. This is due to concentration of flux on the side, however the yellow-orange flash does not show fully from this angle yet it can be studied clearly from Figure 32.

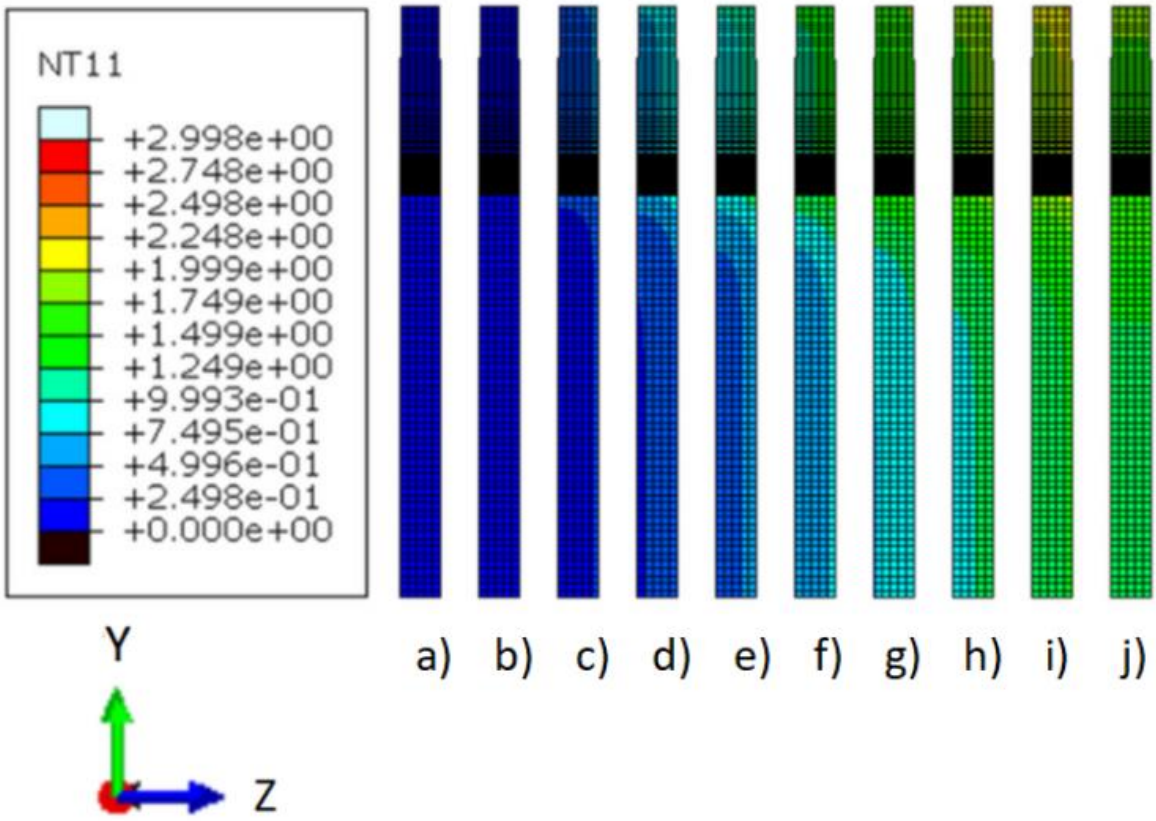

Figure 32: Notched dog bone model with flux load applied, profile view at a) 0s b) 180s c) 240s d) 540s e) 720s f) 1020s g) 1380s h) 1740s i) 1920s j) 2820s

Figure 32 shows a major difference in simulation using flux load method from the boundary condition method. On the notched part in Subfigures h) and i), a higher hydrogen concentration than surroundings is confirmed, but soon it diffuses out evenly as the simulation draws to an end. It seems that the flash with higher hydrogen concentration flux happens on the part where the geometry is not linear and simple.

The simulation results from the boundary condition method and flux load method naturally shows the major difference between them. Generally, they show similar behavior until they reach proximity of the final hydrogen concentration level around time step 1920 then the simulation using flux load method shows a flash of hydrogen concentration that goes as high as over 2.5e+00.

5.2.2 Results: Central hole

The results from simulations conducted on the model with a central hole using both the boundary condition method and the flux method are presented in this section.

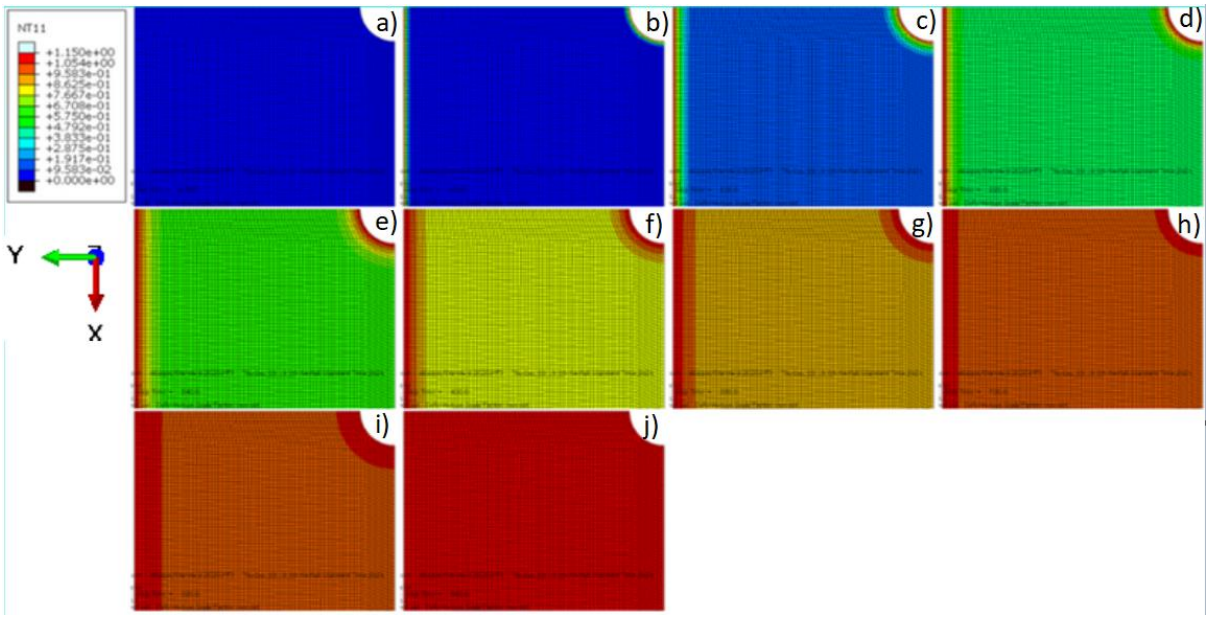

Figure 33: Central hole model, Boundary condition method for the 4 mm diameter hole sample at a) 0s b) 10s c) 100s d) 220s e) 340s f) 460s g) 580s h) 700 i) 820s j) 940s

The boundary condition of higher hydrogen concentration was applied on the surface of the hole (right top corner on each subfigure) and an outer surface of the specimen (left side on each subfigure). From observing the resulting Figure 33, it can be confirmed that the hydrogen diffuses from those two outer surfaces into the inner side. The diffusion happens in a similar manner as in the previous simulation on the 15 mm notched dog bone model, as both of them show the fastest rate of diffusion.

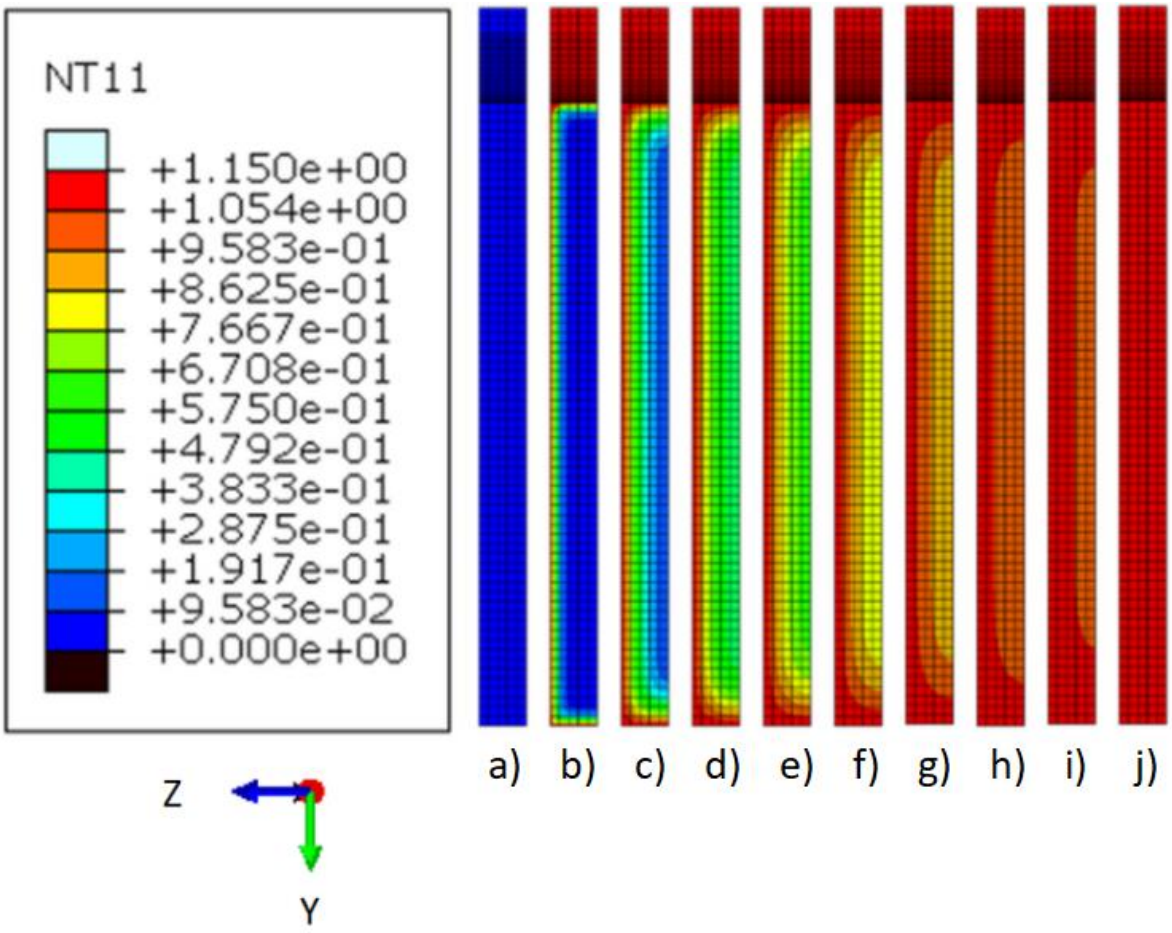

Figure 34: Central hole model, Boundary condition method for the 4 mm diameter hole sample, profile view at a) 0s b) 10s c) 100s d) 220s e) 340s f) 460s g) 580s h) 700 i) 820s j) 940s

In Figure 34, the same result is shown from the angle that illustrates the side of the model. The boundary condition applied on another outer surface and the surface of the hole on the model can be seen from Subfigure b), and the hydrogen is diffused from these surfaces into the inner part of the model until even hydrogen concentration distribution is reached at j).

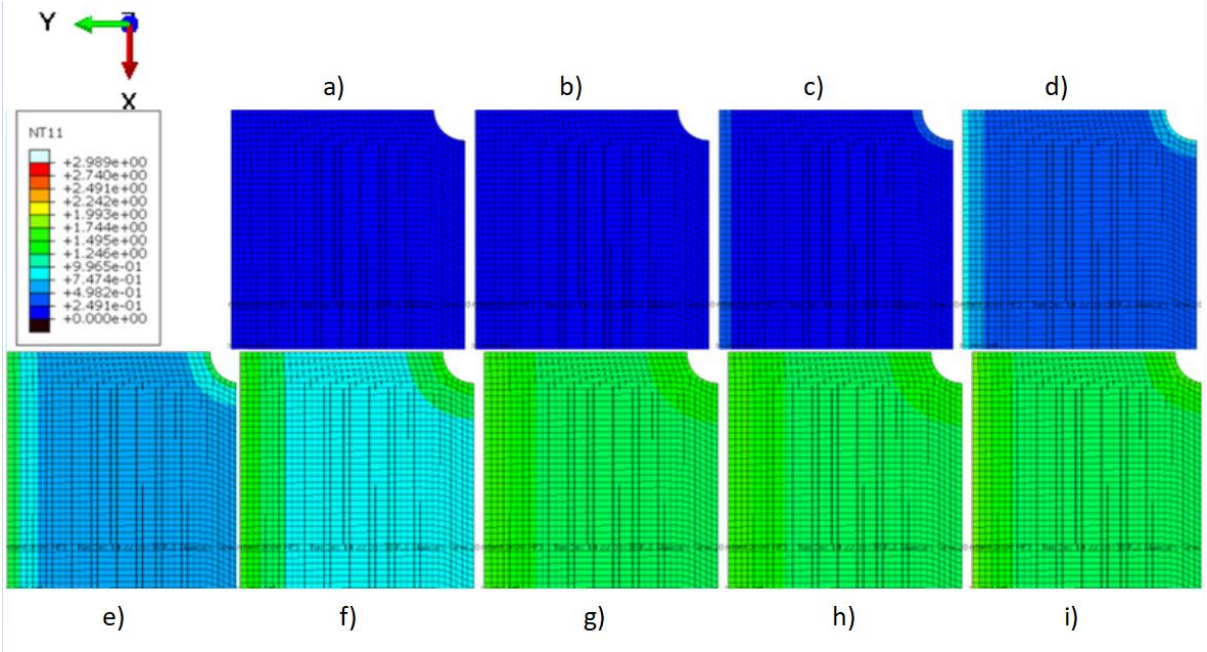

Figure 35: Flux results for the 4mm diameter hole sample at a) 0s b) 60s c) 360s d) 780s e) 1200s f) 1680s g) 2020 h) 2370s i) 3070s

Looking at Figure 35, the flux step is shown in Subfigure a) to f) and diffusion step is shown in Subfigure g) to i). Again, the Figure does not seem to exhibit much difference, except that the values are mapped with different colors now due to concentration of flux on the side. Another viewport of the same sample is shown in the next Figure.

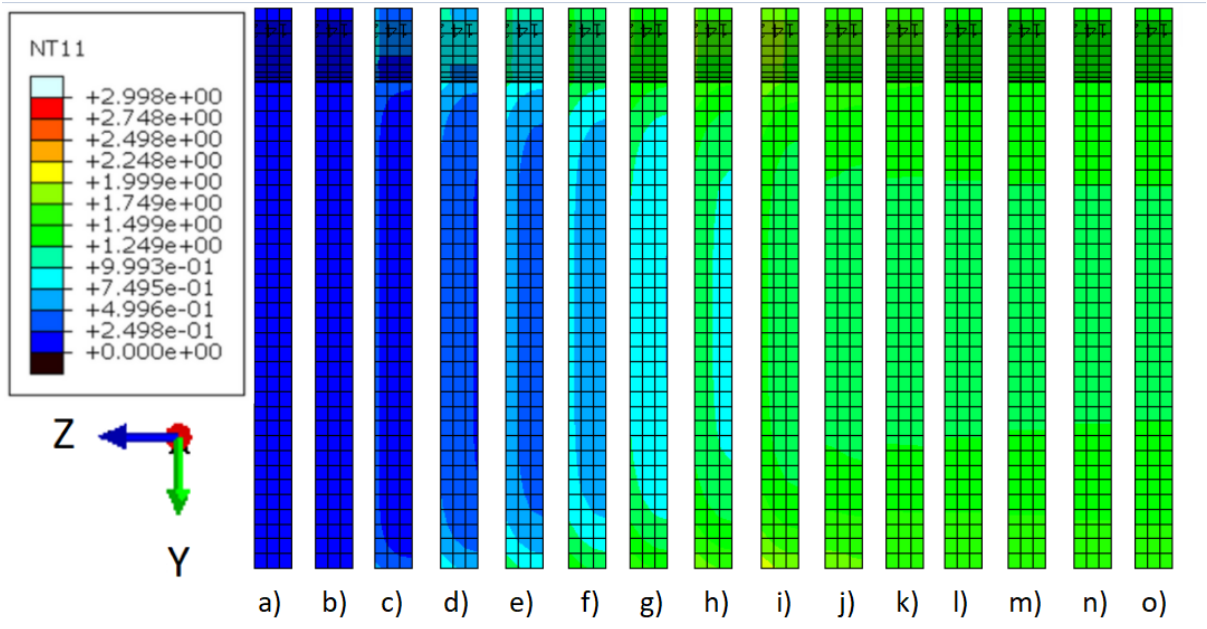

Figure 36: The flux results for the 4 mm diameter hole sample at a) 0s b) 60s c) 240s d) 540s e) 780s f) 1080s g) 1380s h) 1680s i) 1920s j) 2120s k) 2370s l) 2620s m) 2870s n) 3120s o) 3320s

The same simulation is now shown in Figure 36. The subfigures are obtained with more frequent intervals now so that the higher hydrogen concentration on the fraction of the model can be captured properly. The Subfigures a) to g) show the simulation during the flux step. At 1920s the step changes into heat transfer as it reaches the highest hydrogen concentration level. It can be visually confirmed on the top portion of Subfigure i) where a yellow area is showing on the central hole. The higher hydrogen concentration is distributed to other parts and the simulation reaches a uniform concentration after 1920s.

5.2.3 Results: Complex hole geometry

The boundary condition and flux load method results for the complex hole geometry are shown in Figures 37 and 38 respectively.

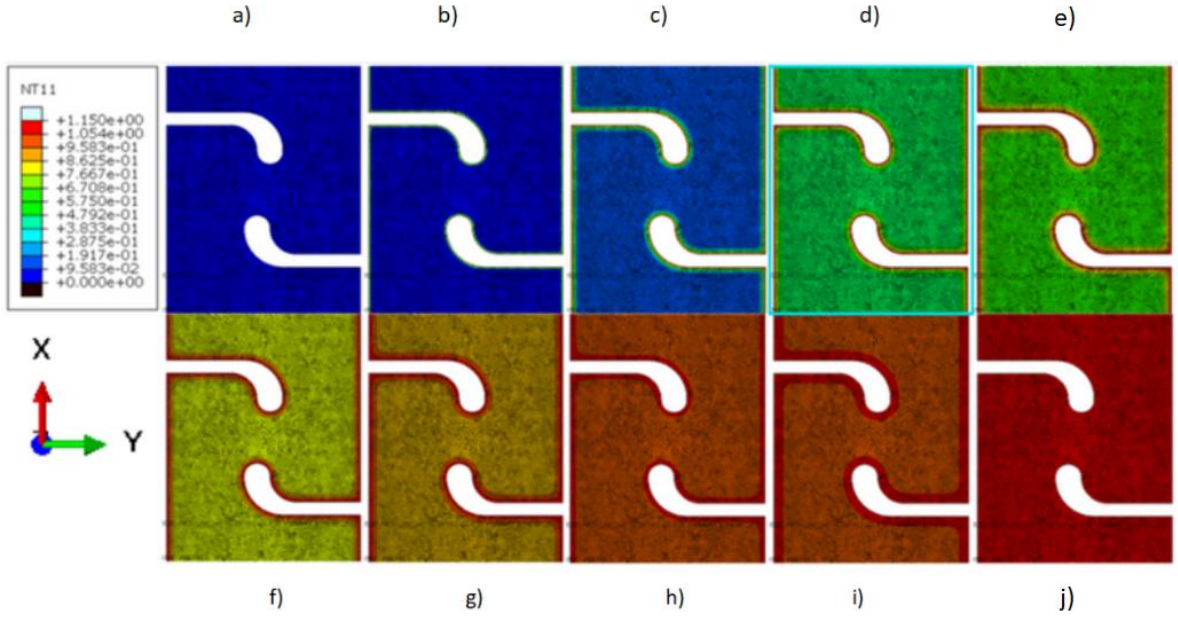

Figure 37: Boundary method results for the complex holes sample at a) 0s b) 20s c) 100s d) 220s e) 350s f) 460s g) 560s h) 700s i) 860s j) 1000s

As Figure 37 shows the boundary maximum that is set at the start of the simulation diffuses into the sample with time till a uniform maximum hydrogen concentration of 1.15 at.ppm is reached. Uniform concentration is reached at about 1000s as is seen in Subfigure j).

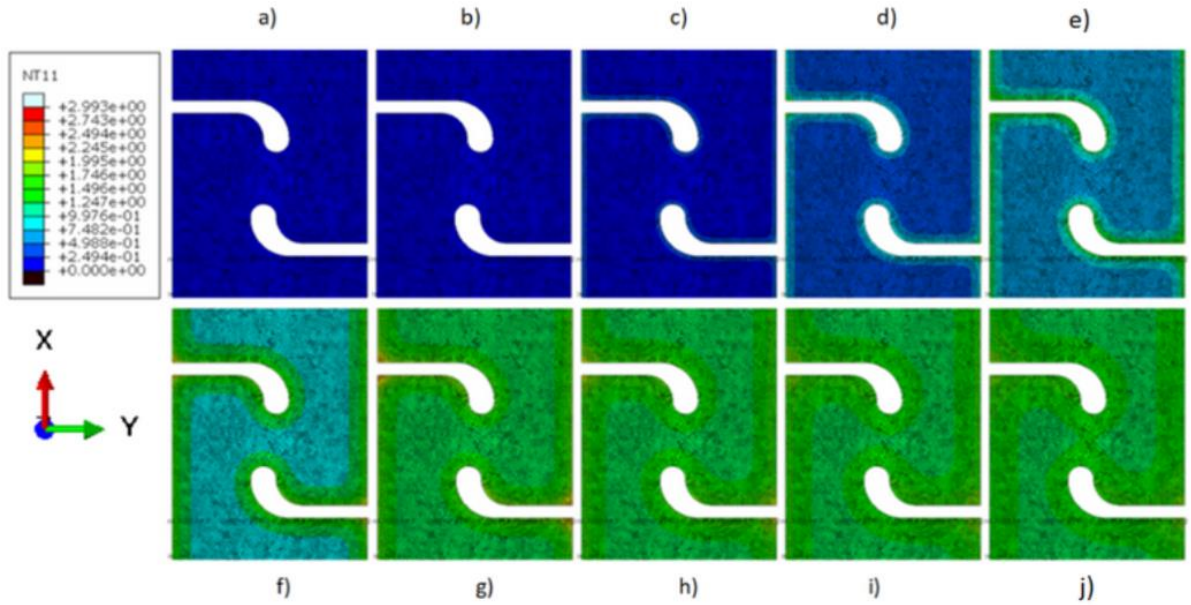

Figure 38: Flux method results for the complex holes sample at a) 0s b) 60s c)180s d) 480s e) 900s f) 1320s g) 1920s h) 2120s i) 3920s j) 6920s

As Figure 38 shows only small specific areas of the sample reach high concentrations of hydrogen. The flux step is shown in Subfigures a) to f). Subfigure g) shows the result of the flux step, therefore it shows the highest concentrations. These areas can be seen in Subfigure g), where a bright red area is located at each corner of the complex hole. Otherwise, the concentration throughout the sample seems to reach a uniform concentration at already Subfigures i) and j) so at time range of 3920-6920s.

5.2.4 Discussion: Three-dimensional simulation

The results for the boundary condition and flux load methods contrast each other quite a lot. The flux load method has occasional higher concentration spots in the sample during the flux step, which diffuse into the sample during the diffusion step. These so-called concentration hot spots were usually located in spots where multiple flux surfaces met such as corners (as was seen in the case of the complex holes sample)

or along edges of surfaces (shown in the notched samples). In contrast, the boundary method produces similar hydrogen diffusion patterns for all geometries. The boundary condition value, that was defined at the start of the simulation, slowly diffuses into the sample till a uniform concentration of said boundary condition value is reached. Therefore, the boundary method does not fully reproduce the actual experimental scenarios since the boundary condition must be set and therefore the final concentration must be known for the boundary method to produce realistic results.

While the boundary condition method has clear limitations, the flux load method also has some possible improvements that could be done. The initial flux value that is input in the simulation depends on the total hydrogen concentration obtained from the TDS experiment. Since the TDS experiment was not conducted for the complicated geometries yet, we were not able to calculate an accurate value for initial flux. Therefore, we used the same value for the simple geometry case in order to replicate the simulation strategy for the complicated geometries. This inaccuracy can be seen in the results since the uniform hydrogen concentration value in the final time step is not equal to 1.15 at.ppm. However, once the correct initial value is obtained, we will get reliable results from these simulations. It should be noted that the simulation model is fully developed, the only required change would be in the initial value, which is a trivial correction.

6. Conclusions and Outlooks

The purpose of this project is to mark the first step in simulating and understanding the hydrogen embrittlement process. Hydrogen embrittlement can negatively impact the mechanical properties of a material by reducing its ductility and accelerating brittle failure, so it is important to understand the mechanism of how this happens. By solving the coupled mechanical-diffusion equation, we can understand the underlying process of how hydrogen influences the mechanical properties of the material. However, by analyzing the diffusion equation, we will get more insight on how hydrogen diffuses through the material, which will serve as the foundation for future studies in this field.

In order to understand the diffusion process of hydrogen through the sample, the analogy between the diffusion and heat transfer equations was made use of to simulate the model in MATLAB and Abaqus. An analytical approach was implemented for one-dimensional case using MATLAB and the same results were achieved through simulation in Abaqus, thus proving our assumptions and procedure were correct. Furthermore, a different simulation strategy following the mass flux concept was implemented which gave results resembling real-life experimental scenarios. The Abaqus simulation strategies were further applied to three-dimensional complex geometries.

The simulation strategy involving boundary conditions is rather ideal, and while it is useful in understanding the diffusion process it does not resemble a real-life case. The mass flux method, on the other hand gives us a uniform concentration at the end of the diffusion process, which is more similar to what we see in experiments. This method also shows us that in certain areas of the specimen like corners or edges especially in the three-dimensional complicated geometries, we find more concentration build-up, which matches our initial assumption that hydrogen diffuses into the material and tends to accumulate in defects or areas of high strain concentration. Due to this reason, for the three-dimensional complex geometries, it would make more sense to model the coupled simulation since we expect the geometry to also factor in and contribute to the stress analysis.

The study presented in this paper can serve as a firm base step for further studies to be done in this field, especially the fully coupled diffusion-mechanical model. Simulating the coupled model will require more time and knowledge about the subject and simulation tools but is an important feat to achieve since it will help us clearly understand the hydrogen embrittlement process. In the coupled modeling, as stress is applied on the material and strain increases, the dislocation density also increases. Since hydrogen concentration is proportional to high strain concentration, this simulation will help us understand how the hydrogen distribution changes quantitatively during the tensile process and explain the mechanism behind hydrogen's influence on the damage property of the material.

7. Personal Evaluation

The Computational Engineering project has been a huge learning experience for all three of us and one of the highlights of our BSc. degree. We were quite excited at the chance to finally do some hands-on research work after 2 years of primarily lectures and assignments. The three of us are close friends, so we were also happy to work together, and doing this project only brought us closer. Through this project, we were able to learn about a completely new topic- hydrogen embrittlement and produce some solid results in this field. We also further improved our coding skills in MATLAB and learnt to use a rather new software, Abaqus. Through our different trials and approaches, we learnt valuable things from our mistakes. In the end, we also learnt to effectively present our results to our supervisors and peers, and write an academic report on our study.

While we did have fun with this project, it did come up with some trouble. Our main regret is that we weren't able to complete the full aim of our project which was the coupled hydrogen charging and mechanical response analysis. This was mainly because we lacked the foundational knowledge about this topic and thus had to learn it from the beginning. We unfortunately ran out of time to fully understand and implement what we had to do. Another major issue we faced was with regard to communication, especially with our advisor. Good communication is vital for the success of any research project, so we were motivated to put in extra effort to communicate with each other properly. We could've also managed our time a little better to avoid pile-up of work in the end. Also, we could've also been more committed towards this project and our work.

Overall, this project course has certainly been fun for us, with its ups and downs. The course had been organized quite well, with less confusion about the practicalities. However, we could've been given slightly more time to familiarize ourselves with the topics, before we had to choose one, in the beginning of the course. The topic and group selection were rather rushed and stressful.

At the end of this project, we would like to express our sincerest gratitude towards our advisor, Ms. Jiaojiao Wu for all her help, support and guidance throughout the course of this project. Also, a big thanks to our supervisor, prof. Junhe Lian for giving us the opportunity to do this project and believing in us.

8. References

[1] T. Scott, A. Troiano, Interstitials and fracture of metals, Nature 185 (4710) (1960) 372–373, http://dx.doi.org/10.1038/185372a0.

[2] H. Johnson, A. Troiano, Crack initiation in hydrogenated steel, Nature 179 (4563) (1957) 777, http://dx.doi.org/10.1038/179777a0.

[3] T. Mohr, A. Troiano, R. Hehemann, Stress corrosion cracking of ferritic stainless steels in chloride solutions, Corrosion 37 (4) (1981) 199–208.

[4] R. Garber, I. Bernstein, A. Thompson, Hydrogen assisted ductile fracture of spheroidized carbon steels, Metall. Trans. A 12 (2) (1981) 225–234, http://dx. doi.org/10.1007/BF02655195

[5] Hydrogen Embrittlement - A Serious Challenge for the Industry, https://www.4realsim.com/hydrogen-embrittlement/. Accessed on 23/12/2021

[6] O. Barrera, E. Tarleton, H.W. Tang, A.C.F. Cocks, Modelling the coupling between hydrogen diffusion and the mechanical behaviour of metals, Computational Materials Science 122 (2016) 219-228, https://doi.org/10.1016/j.commatsci.2016.05.030

[7] Wei Zhang, Evaluation of Susceptibility to Hydrogen Embrittlement—A Rising Step Load Testing Method, Materials Sciences and Applications, Vol. 7 No. 8, August 2016, DOI: 10.4236/msa.2016.78035

[8] Dini, J.W. (1993) Electrodeposition: The Materials Science of Coatings and Substrates. Noyes Publications, Westwood, NJ, USA.

[9] Helmut, K. (2003) Corrosion of Metals: Physicochemical Principles and Current Problems. Springer, Berlin, New York.

[10] Raymond, L. (1988) Hydrogen Embrittlement: Prevention and Control. American Society for Testing and Materials, Philadelphia, PA.

[11] Timmins, P.F. (1997) Solutions to Hydrogen Attack in Steels. ASM International, Materials Park, OH.

[12] Raymond, L. (1998) The Susceptibility of Fasteners to Hydrogen Embrittlement and Stress Corrosion Cracking. In: Bickford, J. and Nassar, S., Eds., Handbook of Bolts and Bolted Joints, Chap. 39, Marcel Decker, Inc., New York, 723.

[13] Tyler, P.S., Levy, M. and Raymond, L. (1991) Investigation of the Conditions for Crack Propagation and Arrest under Cathodic Polarization by Rising Step Load Bend Testing. Corrosion, 47, 82-86.
http://dx.doi.org/10.5006/1.3585857

[14] Raymond, L. and Crumly, W.R. (1982) Accelerated, Low-Cost Test Method for Measuring the Susceptibility of HY-Steels to Hydrogen Embrittlement. Proceedings of the First International Conference on Current Solutions to Hydrogen Embrittlement in Steels, Washington DC, 1-5 November 1982, 477.

[15] National Materials Advisory Board (1976) Rapid Inexpensive Tests for Determining Fracture Toughness. NMAB 328, National Academy of Sciences, Washington DC.

[16] W. H. Johnson: Proceedings of the Royal Society of London, 23 (1875) 168–179.

[17] Hydrogen-Materials Interactions Proceedings of the 2012 International Hydrogen Conference

[18] S. Wang, M.L. Martin, I.M. Robertson, and P. Sofronis: unpublished research, 2015.

[19] I. Robertson, The effect of hydrogen on dislocation dynamics, Eng. Fract. Mech. 64 (5) (1999) 649–673, http://dx.doi.org/10.1016/S0013-7944(99)00094-6. cited By 51.

[20] H.K. Birnbaum, P. Sofronis, Mater. Sci. Eng. A. 1993, *A176*, 191-202.

[21] C. D. Beachem, Metall. Trans A 1972, *3*, 437 - 451.

[22] J. K. Lin, and R. A. Oriani, Acta Metall. 1983, *31* (7), 1071-1077

[23] R. A. Oriani, and P. H. Josephic, Acta Metall. 1979, *27*, 997-1005.

[24] R. A. Oriani, and P. H. Josephic, Scripta Metall. 1979, *13* (6), 469-471.

[25] Fick's Second Law and Non Steady State Diffusion, https://www.youtube.com/watch?v=SCWOvR3s3tU, Accessed on 16/12/2021

[26] Shusaku TAKAGI, Yuki TOJI, Application of NH4SCN Aqueous Solution to Hydrogen Embrittlement Resistance Evaluation of Ultra-high Strength Steels, ISIJ International, Vol. 52 (2012), No. 2, pp. 329–331

[27] Eric Fangnon, Evgenii Malitckii, Yuriy Yagodzinskyy, Pedro Vilaça, Improved Accuracy of Thermal Desorption Spectroscopy by Specimen Cooling during Measurement of Hydrogen Concentration in a High-Strength Steel, Materials 2020, 13, 1252; doi:10.3390/ma13051252

[28] Crank, J.; Nicolson, P. (1947). "A practical method for numerical evaluation of solutions of partial differential equations of the heat conduction type". *Proc. Camb. Phil. Soc*. **43** (1): 50–67. doi:10.1017/S0305004100023197

[29] Robertson, I.M., Sofronis, P., Nagao, A. et al. Hydrogen Embrittlement Understood. Metall Mater Trans B 46, 1085-1103 (2015).https://doi.org/10.1007/s11663-015-0325-y

9. Appendix

Appendix A: One dimensional MATLAB code

```
D=3.07*10^-4; %diffusion coefficient mm^2/s
T = readmatrix('matlab_5.xlsx');
%%%%%%%%% Define the x-domain and x-grid %%%%%%%%%%%%%%%%
Lx=0.5; %domain mm
Nx=14;
nx=Nx+1; %number of nodes
dx=Lx/Nx;
x=((0:Nx)*dx);

%%%%%%%%% Time steps %%%%%%%%%%%%%%%%%%%%%%%%%

nsteps=60;
nout= 5;
dt= 5;
alpha=dt*D/dx^2;


%%%%%%%%% Construct the matrix %%%%%%%%%%%%%%%%%%%

diagonals=[2*(1+alpha)*ones(nx,1), -alpha*ones(nx,2)];
A=spdiags(diagonals,[0 -1 1], nx, nx);
I=speye(nx);
A ([1 nx],:) = I([1 nx],:);

%%%%%%%%% Define initial conditions and plot %%%%%%%%%%%%%%%%%%

u=zeros(1,nx);
u(1)=1;
u=u';

%%%%%%%%% Advanced solution and plot %%%%%%%%%%%%%%%%%%
for m=1:nsteps
b=[2.3;[alpha*u(1:nx-2)+2*(1-alpha)*u(2:nx-1)+alpha*u(3:nx)]; 0];
u=A\b;
if mod(m,nout)== 0, plot(x,u,'b'); hold on; end % matlab!
end
[m,n] = size(T);
xlabel('Thickness direction (z-axis), mm');
ylabel('Hydrogen concentration, at.ppm');
for t = 1:(n/2)-3
    plot(T(:,t+(t-1)), T(:,t+t), 'r');hold on; % red is abaqus!
end
legend('Matlab', 'Abaqus');
```

Appendix B: MATLAB Code to Calculate Total Hydrogen Concentration from TDS Experiment

```
% Read the data from the file
x1 = xlsread( 'CP1000_HC_TDS_Original.xlsx', 'CP1000_H_04' ,'A3:A8203');
y1 =xlsread( 'CP1000_HC_TDS_Original.xlsx', 'CP1000_H_04' ,'B3:B8203');

%Plot original data
plot(x1, y1)

%Split graph
newx1 = x1(1:find(x1 == 320));
newy1 = y1(1:find(x1 == 320));
newx2 = x1(find(x1 == 370):find(x1 == 555));
newy2 = y1(find(x1 == 370):find(x1 == 555));
newx3 = x1(find(x1 == 555):find(x1 == 802));
newy3 = y1(find(x1 == 555):find(x1 == 802));
newx4 = x1(find(x1 == 802):length(x1));
newy4 = y1(find(x1 == 802):length(x1));

%Gaussian curves

%Curve 1
a11 =    0.003055;
b11 =       303.1;
c11 =      0.2219;
a12 =     0.06839;
b12 =       207.9;
c12 =       129.7;
xx1 = -100:0.1:500;
f1 =  a11*exp(-((xx1-b11)/c11).^2) + a12*exp(-((xx1-b12)/c12).^2);
f11 = @(xx1) a11*exp(-((xx1-b11)/c11).^2) + a12*exp(-((xx1-b12)/c12).^2);
area1 = integral(f11,301,349.2);

%Curve 2
a21 =     0.05322;
b21 =       424.2;
c21 =       77.36;
a22 =    -0.01523;
b22 =       484.3;
c22 =       33.53;
xx2 = 250:0.1:600;
f2 =  a21*exp(-((xx2-b21)/c21).^2) + a22*exp(-((xx2-b22)/c22).^2);
f22 = @(xx2) a21*exp(-((xx2-b21)/c21).^2) + a22*exp(-((xx2-b22)/c22).^2);
area2 = integral(f22,349.2,557);

%Curve 3
a31 =     0.01685;
b31 =       684.4;
c31 =       9.945;
a32 =     0.01846;
b32 =       682.1;
c32 =       39.41;
a33 =     0.01271;
```

```
b33 =       706.7;
c33 =       120.1;
xx3 = 475:0.1:925;
f3 = a31*exp(-((xx3-b31)/c31).^2) + a32*exp(-((xx3-b32)/c32).^2) + a33*exp(-((xx3-
b33)/c33).^2);
f33 = @(xx3) a31*exp(-((xx3-b31)/c31).^2) + a32*exp(-((xx3-b32)/c32).^2) +
a33*exp(-((xx3-b33)/c33).^2);
area3 = integral(f33,557,797.1);

%Curve 4
a41 =    0.007293;
b41 =       820.1;
c41 =       226.3;
a42 =  -6.328e-05;
b42 =       808.1;
c42 =       3.278;
xx4 = 400:0.1:1300;
f4 = a41*exp(-((xx4-b41)/c41).^2) + a42*exp(-((xx4-b42)/c42).^2);
f44 =  @(xx4) a41*exp(-((xx4-b41)/c41).^2) + a42*exp(-((xx4-b42)/c42).^2);
area4 = integral(f44,797.1,1121);

figure;
plot(x1, y1);
hold on;
plot(xx1,f1, 'LineWidth', 2);
plot(xx2,f2, 'LineWidth', 2);
plot(xx3,f3, 'LineWidth', 2);
plot(xx4,f4, 'LineWidth', 2);
xlabel('Temperature (K)');
ylabel('Hydrogen Desorption Rate (ppm/s)')
hold off;

totalarea = area1+area2+area3+area4;
cH = 0.1 * totalarea;
disp(cH)
```